EXPLORING THE ROLE OF CHEMOTHERAPY-INDUCED ANASTASIS IN TRIPLE-NEGATIVE BREAST CANCER

by

Jennifer Nagel

B.Sc., Memorial University of Newfoundland, 2016

A THESIS SUBMITTED IN PARTIAL FULFILLMENT OF

THE REQUIREMENTS FOR THE DEGREE OF

MASTER OF SCIENCE

in

THE FACULTY OF GRADUATE AND POSTDOCTORAL STUDIES

(Biochemistry and Molecular Biology)

THE UNIVERSITY OF BRITISH COLUMBIA

(Vancouver)

September 2019

The following individuals certify that they have read, and recommend to the Faculty of Graduate and Postdoctoral Studies for acceptance, a thesis entitled:

EXPLORING THE ROLE OF CHEMOTHERAPY-INDUCED ANASTASIS IN TRIPLE-NEGATIVE BREAST CANCER

submitted by Jennifer Martha Nagel in partial fulfillment of the requirements for

the degree of Master of Science

in Biochemistry and Molecular Biology

Examining Committee:

Dr. Shoukat Dedhar
Supervisor

Dr. Calvin Roskelley
Supervisory Committee Member

Dr. Chris Overall
Supervisory Committee Member

Dr. Sharon Gorski
Additional Examiner

Abstract

Triple-negative breast cancer (TNBC), is an aggressive and metastatic variant that lacks relevant treatment-targeted receptors. In addition, resistance to cytotoxic chemotherapeutic drugs is a common attribute of these cells, although little is known about how it is acquired. My hypothesis is that “Anastasis”, a reversal of end-stage apoptosis demarked by caspase-3 (Cas3) cleavage plays a role in drug resistance and cancer progression. Anastasis has been observed in many cell types, including cancer, however, its role in response to apoptotic stimuli is poorly understood, especially concerning its induction by clinically relevant chemotherapy agents. To test the above hypothesis, I used a GFP-tagged Cas3 reporter in order to measure DEVDase (pro-caspase) activity, indicating the level of Cas3 activation indirectly. This allowed for the selection of living, apoptotic cells using fluorescent activated cell sorting (FACS), whereby post-anastatic cells survived chemotherapy-induced apoptosis upon drug removal. While these cells do not appear phenotypically different, it was shown that they are more resistant to the original treatment, possess increased DNA damage, are more invasive, migratory, and metastatic, as well as more metabolically robust. Mechanistically, I determined that these cells produce a truncated caspase-3 isoform (Cas3s) that prevents apoptosome assembly early in the recovery stages of anastasis and long after its completion. Additionally, levels of native Cas3 remained unchanged during recovery and a decrease in Cas3 activation was observed upon treatment. Furthermore, a phenotypic characteristic of the post-anastatic cells revealed a significant up-regulation of epithelial-mesenchymal transition (EMT) and hypoxia stress markers. Inhibition of one of the up-regulated proteins, integrin-linked kinase (ILK) resulted in re-sensitization to chemotherapy

treatment, a decrease in migration, as well as a dampening of the enhanced metabolic activity. These findings support a potential role for anastasis as a novel mechanism for resistance in TNBC and provides mechanistic insight into its role in tumor cell biology, that which has not been previously described.

Lay Summary

Breast cancer (BC) arises when a cell's DNA becomes damaged, leading to changes in activity within the cell. BC subtypes have unique characteristics that can be exploited through the application of different clinical treatments, however, triple-negative breast cancer (TNBC) is aggressive and difficult to treat as it lacks these specific therapeutic targets. Moreover, TNBC recurs at high rates in previously diagnosed patients and is often resistant to treatment, often in cases where it has spread to distant sites in the body. Cancer cells that spread from one area of the body to another undergo a structural change, allowing them to become more migratory and invasive. It is proposed that a reversal in the cell-death program, initiated in times of extreme stress or damage, can cause further changes to the cancer's DNA; leading to a decrease in treatment responsiveness. This research has identified potential targets for reversing drug resistance and provides new insight into the mechanism through which drug resistance propagates in TNBC.

Preface

This master's thesis is presented in four chapters. All experiments described in Chapter 3 were conceived and designed by Jennifer Nagel, Dr. Shoukat Dedhar, Dr. Paul MacDonald. All experiments were carried out by Jennifer Nagel.

Fluorescent activated cell sorting (FACS) described in Chapter 3 was carried out by the Flow Cytometry Core Facility in the TFL of the BC Cancer Research Centre (Vancouver, BC, Canada). The plasmid for the GC3AI Cas3 reporter used in these experiments was provided by Dr. Denise Montell at the University of California (Santa Barbara, CA, USA).

Jordan Gillespie performed the *in vivo* experiments described in Chapter 2 and 3. Animal studies and procedures were performed in accordance with protocols approved by the Institution Animal Care Committee at the BC Cancer Research Centre (Vancouver, BC, Canada) associated with protocol number: A18-0058; under the project title "Evaluation of growth kinetics of Sum159pt and Sum159pt/A cells in mice".

Table of Contents

List of Tables

List of Figures

List of Symbols

α	alpha
β	beta
µ	micro
©	copyright
™	trademark
≤	less than or equal to

List of Abbreviations

AC	Anastasis treated with cisplatin
AP	Anastasis treated with paclitaxel
BC	breast cancer
BCCRC	BC Cancer Research Centre
BCL2	B-cell lymphoma 2
BSA	bovine serum albumin
Cas3	caspase-3
Cas3s	caspase-3s (isoform)
CNS	central nervous system
DAPI	4′,6-diamidino-2-phenylindole (DNA stain)
DCIS	ductal carcinoma *in situ*
DMEM	Dulbecco's modified Eagle medium
DMSO	dimethyl sulfoxide
DNA	deoxyribonucleic acid
DS	double-stranded
ECM	extracellular matrix
EGF	epidermal growth factor
EMT	Epithelial-mesenchymal transition
ER	estrogen receptor
FACS	fluorescence activated cell sorting
FBS	fetal bovine serum

FCCF	Flow Cytometry Core Facility
GFP	green fluorescent protein
h	hour(s)
HER2	human epidermal growth factor-2 receptor
HIF-1	hypoxia inducible factor-1
IAP	inhibitors of apoptosis
IDC	invasive ductal carcinoma
ILK	integrin-linked kinase
kDa	kilodalton(s)
L	liter(s)
M	molar
m	meter(s)
MCT4	monocarboxylate transporter-4
mins	minute(s)
ml	milliliter(s)
MOPS	3-(N-morpholino)propanesulfonic acid buffer
n	nano
NEAA	non-essential amino acids
NSG	NOD.CB17-Prkdcscid/J-IL-2R-/-
PAGE	polyacrylamide gel electrophoresis
PBS	phosphate buffered saline
PFA	paraformalin
PR	progesterone receptor

PI	propidium iodide
PI3K	PI-3 kinase
RIPA	radioimmunoprecipitation buffer
RNA	ribonucleic acid
RNAseq	RNA sequencing
RT	room temperature
s	second(s)
SDS	sodium dodecyl sulfate
SS	single-stranded
TBST	Tris-buffered saline and Tween 20
TFL	Terry Fox laboratory
TNBC	Triple-negative breast cancer
TNF	tumor necrosis factor
V	volts
WB	western blot
WT	wild-type

Acknowledgements

To begin with, I would like to extend my most sincere gratitude to my supervisor, Dr. Shoukat Dedhar, for not only giving me the opportunity to complete my master's research in his lab; but for also allowing me to take on a project that was very much pushing the leading edge in this niche of cancer research. It has truly been a privilege and an experience I will carry with me throughout the rest of my educational training and career.

Additionally, I would like to thank Dedhar lab members Shannon Awrey, Dr. Shawn Chafe, and Dr. Mridula Swayampakula, whom not only took the time to teach me invaluable scientific techniques when I first entered the lab, but also took part in many discussions regarding interpretation of data and offered valuable insight.

I would also like to thank all of the lab members: Shannon Awrey, Dr. Shawn Chafe, Dr. Mridula Swayampakula, Dr. Wells Brown, Dr. Paul MacDonald, Oksana Nemirovsky, Geetha Venkateswaran, and Jordan Gillespie, for making long days shorter with fun banter that I hold very dear to my heart. You all gave me a reason to look forward to coming to lab every day, thank you for being kind, funny, and patient.

I would also like to extend my most sincere thanks to my committee members: Dr. Chris Overall and Dr. Calvin Roskelley for their guidance and enthusiasm in my research.

Finally, I would like to thank those closest to me who provided emotional support. Thank you to Rizza Umali, Shanna Stacey, and my sister Lindsey Nagel, for keeping me sane with vent sessions, funny messages, and much needed phone calls. You are all so important to me and I am in awe of your strength and accomplishments. I would also like to thank my parents for believing in me when I really didn't think I could do it, and who built me up when I felt I was falling short.

I dedicate this work to all the scientists' and doctors working tirelessly to better the treatment for all cancer patients alike. I am inspired by your drive, work ethic, intelligence, and compassion. Thank you for making it your life's mission to better the lives of others.

Chapter 1: Introduction

1.1 Breast Cancer

Breast cancer (BC) is one of the most prevalent cancers among Canadian women and is the second leading cause of death among these women (Canadian Cancer Society, 2019). It is estimated that in 2017, 26,300 women were diagnosed, and 5,000 women succumbed to the disease (Canadian Cancer Society, 2019). BC comprises many subtypes that begin formation in the duct of the breast tissue, which can migrate into the glandular tissue and typically go on to metastasize to exterior regions including the lymph nodes, lung, liver, and the bone marrow (Weigelt, B. et al., 2005).

1.1.1 Classification of subtypes

BC tumors are heterogeneous cellular landscapes with varying molecular profiles that determine a patient's outcome and response to different available clinical therapies (Weigelt et al., 2008). BC can be classified by its genetic profile, the tissue type/origin, and the pattern of growth in the breast tissue. From a physiological viewpoint, there are two major classifications: invasive (*in situ*) and non-invasive. Non-invasive ductal carcinoma *in situ* (DCIS) propagates and remains in the duct where it originated, and accounts for 20% of all breast cancers diagnosed (Muggerud et al., 2010). Cases of DCIS are associated with a more favorable outcome, however, regrettably there is a 50% chance it will transform into an IDC, an event that is especially prevalent in cases of relapse (Muggerud et al., 2010). The molecular classification of DCIS includes luminal A and

B, basal-like, normal-like, estrogen receptor (ER)-negative, ER-positive, progesterone (PR)-negative, high-grade, and HER-2-positive (Muggerud et al., 2010). Invasive ductal carcinoma (IDC), as the name suggests, invades out of the duct of origin, into the surrounding breast tissue, comprising 50-80% of all cases diagnosed (Weigelt et al., 2008). This can be broken down further into other subcategories as seen in Figure 1.1. The molecular classification of IDC includes subtypes such as human epidermal growth factor receptor-2 (HER-2) positive, a tyrosine kinase; luminal, and basal-like (Weigelt et al., 2008).

The genetic and molecular profiles of BC are typically evaluated using receptor status and the presence of specific genetic mutations, which may be hereditary or autosomal in origin. The most common genetic mutations can be found in Table 1.1. Genetic mutations in BC and many cancer types are most commonly oncogenes or tumor suppressors that regulate genome stability and cellular growth (Lodewyk F. A. et al., 2002; Saal, L. H. et al., 2008; Hu, X. et al., 2009). The most common receptors considered for treatment purposes are hormonal, such as estrogen and progesterone, and HER-2 status. The status of these receptors not only dictates the type of treatment used but a tumor's response to it, as well (Hu, X. et al., 2009; Dunnwald, L. K. et al., 2007). As a result, receptor status can predict the aggressive nature of a molecular and histological cancer subtype.

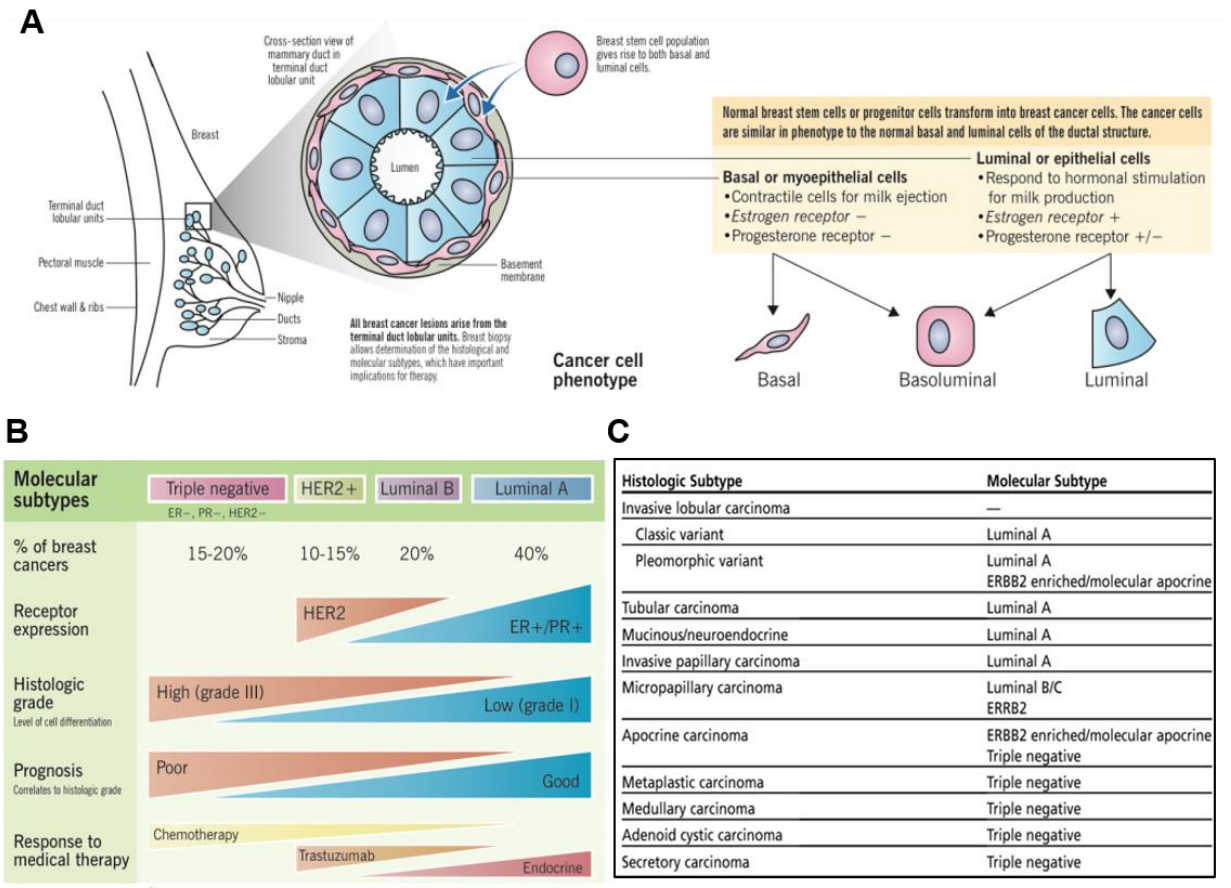

Histologic Subtype	Molecular Subtype
Invasive lobular carcinoma	—
Classic variant	Luminal A
Pleomorphic variant	Luminal A ERBB2 enriched/molecular apocrine
Tubular carcinoma	Luminal A
Mucinous/neuroendocrine	Luminal A
Invasive papillary carcinoma	Luminal A
Micropapillary carcinoma	Luminal B/C ERRB2
Apocrine carcinoma	ERBB2 enriched/molecular apocrine Triple negative
Metaplastic carcinoma	Triple negative
Medullary carcinoma	Triple negative
Adenoid cystic carcinoma	Triple negative
Secretory carcinoma	Triple negative

Figure 1.1 Molecular subtypes of breast cancer and their associated histological subtypes. (A) Image depicting the anatomy of the breast and how that relates to the molecular and histological classification of breast cancer. (B) Table depicting the main characteristics of previously established molecular subtypes of breast cancer. (C) Table depicting the link between molecular and histological subtypes. Figure is modified from "Breast Cancer – McMaster Pathophysiology Review" and "Refinement of breast cancer classification by molecular characterization of histological special types" (Wong, E et al., 2012; Weigelt, B et al., 2008).

Table 1.1 Common breast cancer oncogenes and tumor suppressors

Tumor suppressor genes	Function	Oncogenes	Function
p53	Induces cell-cell cycle arrest and triggers apoptosis	*c-myc*	Transcription factor, involved in proliferation
BRCA-1	DNA repair pathway	*ERB2/HER-2*	Tyrosine kinase receptor, no known ligand
BRCA-2	DNA repair pathway	*Ras*	GTPase, involved in cell proliferation, differentiation, and migration
PTEN	Phosphatase, negative regulator of AKT	*PI3K*	Kinase, involved in cell growth, proliferation, differentiation, and migration
pRb	Retinoblastoma gene, represses cell cycle and inhibits translation	*AKT*	Serine/threonine-kinase, involved in glucose metabolism, proliferation, and apoptosis
ATM	Checkpoint kinase, activates CHK2		

Data supplied from (Osborne, C et al., 2004; Lee, E et al., 2010).

1.1.1.1 Triple-negative breast cancer

While treatment has advanced in the last 30 years by providing therapies that better target varying molecular profiles, triple-negative breast cancer (TNBC), comprising 12-24% of all BCs diagnosed, still carries with it a very poor prognosis (Bosch, A. et al., 2010; O'Reilly, E. A. et al., 2015; Chang, A. et al., 2011). TNBC is defined as a basal-like subtype of breast cancer, due to its similarity to cells outside of the lumen and in the surrounding glandular tissue. TNBC, characterized by tumors that are ER-negative, PR-negative, and HER-2-negative, is particularly aggressive and often metastatic. It is exceedingly challenging to treat as it lacks all above-mentioned therapeutic targets, is often chemoresistant, and often recurs at a high-rate in previously diagnosed patients (Bosch, A. et al., 2010; O'Reilly, E. A. et al., 2015; Chang, A. et al., 2011). Therefore, it is critical to investigate the key players of the tumor microenvironment in order to understand how this affects treatment response.

1.2 Tumor microenvironments

Tumors are a bionetwork of cells that not only interact with each other but also with their environment, making it a dynamic and heterogeneous landscape. In order to maintain homeostasis and propagate in a hostile environment, tumor cells must be able to respond to internal and external stressors accordingly. The tumor microenvironment describes the discreet niches within the tumor, consisting of different immune cell landscapes, blood vessels, metabolism, cell type, oxygen tension and nutrient availability (Figure 1.2). All of this in combination dictates how a tumor behaves and responds to therapy (Kenny, P. A. et al., 2007;

Mbeunkui, F., & Johann, D. J., 2009; Fukumura, D., & Jain, R. K., 2007). Major changes in the cytoskeletal and transcriptional machinery is one way a cell may adapt to a hostile environment.

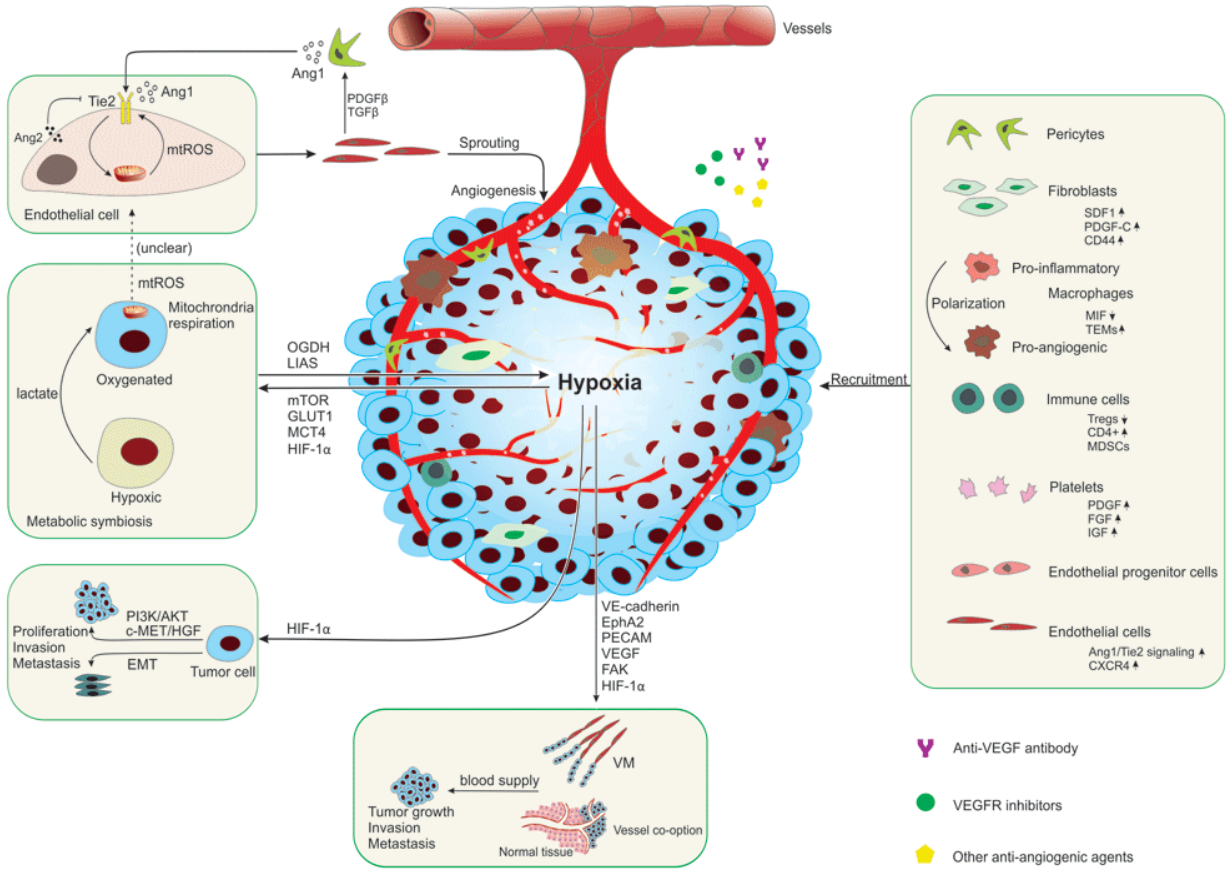

Figure 1.2 Heterogeneous and dynamic nature of the tumor microenvironment
Schematic depicting the potential factors that can influence the tumor landscape, including hypoxia, metabolism, epithelial-mesenchymal transition (EMT), angiogenesis, and immune cells. Figure adapted from "The role of tumor microenvironment in resistance to anti-angiogenic therapy" (Ma et al., 2018).

1.2.1 Epithelial-mesenchymal transition and metastasis

Epithelial-mesenchymal transition (EMT) is an essential mechanism that transpires in a regulated manner to drive events such as gastrulation, organogenesis, and tissue repair; playing a pivotal role not only during embryogenesis but throughout life as well (Liu, T. et al., 2010; Tam, P. P. L., & Behringer, R. R., 1997; Yang, J., & Weinberg, R. A., 2008; Kalluri, R., & Weinberg, R. A., 2009). However, EMT is also a method by which cancer cells lose their polarity, become more spindle-like, and take on more migratory and invasive behaviors (Fig. 1.3) (Timmerman, L. A. et al., 2004). In fact, it is believed to facilitate their progression into new microenvironments, though EMT is not exclusively required for metastasis to occur (Fischer, Kari R. et al., 2015; Creighton, C. J. et al., 2010).

Metastasis is a mechanism that propels cells from a primary tumor to a new, secondary site where a new tumor may form (Fischer, K. R. et al., 2015; Mehlen, P., & Puisieux, A., 2006). It is associated with poor patient outcome, causing the 5-year survival rate to drop from 90% to a staggering 20%; in fact, 90% of therapies fail to treat metastatic cancer due to chemoresistance (O'Reilly, E. A. et al., 2015; Fischer, K. R. et al., 2015). Moreover, genes that drive EMT show an increased presence in invasive and metastatic breast cancer, and as a result, they are potentially implicated in the acquisition of resistance (Fischer, K. R. et al., 2015; Cheng, G. Z. et al., 2007).

EMT is a process that requires a shift from a keratin-rich matrix to one abundant in the protein filament vimentin, the cytoskeletal composition of mesenchymal cells (Hinoshita, E. et al.,

2000). E-cadherin, an adhesion molecule found in epithelial cells, decreases when an EMT event occurs, and its suppression is driven by transcription factors such as, snail, slug, twist, and the protein vimentin ((Singhai, R et al., 2011; Cheng, G. Z et al., 2007). One regulator of these transcription factors is integrin-linked kinase (ILK), a focal adhesion protein involved in modulating multiple signal transduction pathways that has been shown to mediate the suppression of e-cadherin through the transcription of snail (Cheng, G. Z. et al., 2007, Serrano, I. et al., 2013). Lastly, twist, a helix-loop transcription factor, promotes the invasive and migratory behaviors associated with EMT; furthermore, twist has been linked to the heightened expression of endothelial growth factors (EGF), angiogenesis, chromosome instability, and metastasis. Twist has also been implicated in the acquisition of paclitaxel resistance in BC, although it is not known how this occurs (Fischer, K. R. et al., 2015; Martin, T. A. et al., 2005). Interestingly, twist is not only found to be a downstream player in EMT but also in the downstream regulation of hypoxia.

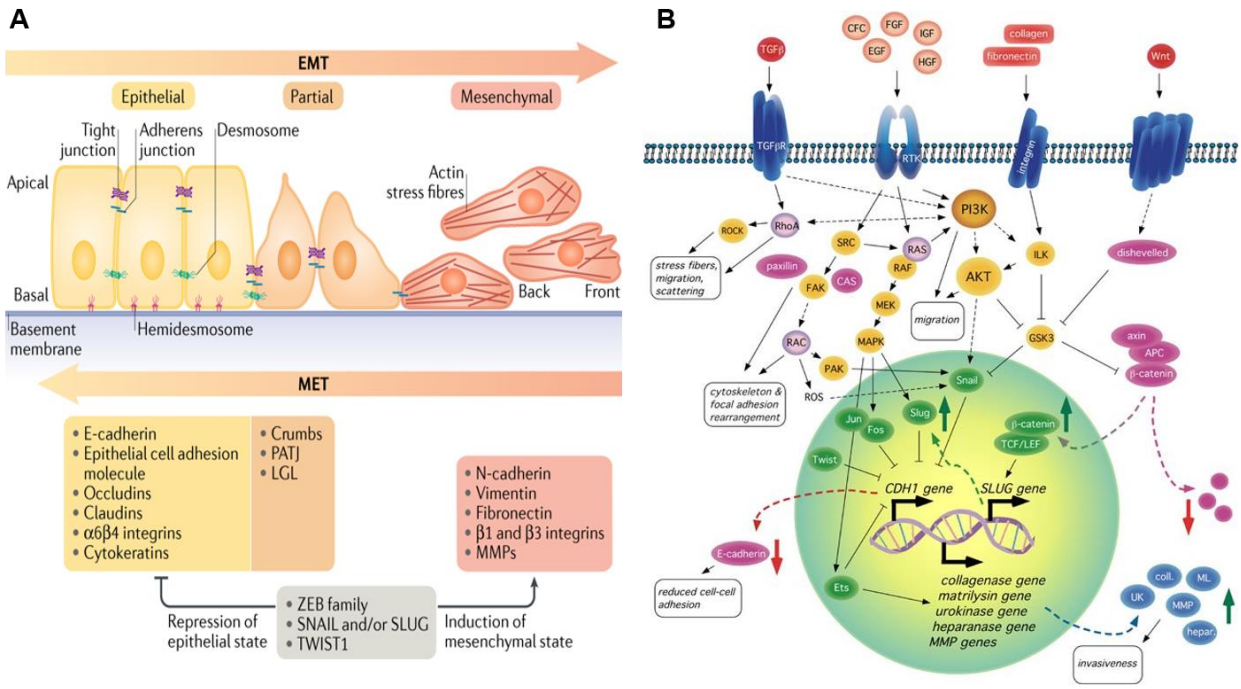

Fig. 1.3 Mechanism of epithelial mesenchymal transition (A) Prior to an EMT event, epithelial cells (*left*) possess tight-junctions and present with apical-basal cellular structure. The cells can transition to either a partial EMT (*center*) where some intercellular interactions are maintained, to a full EMT where cells are completely mesenchymal (*right*). (B) Figure is modified from "New insights into the mechanisms of epithelial–mesenchymal transition and implications for cancer" and "Epithelial-mesenchymal transition in development and cancer: Role of phosphatidylinositol 3′ kinase/AKT pathways" (Dongre, A., & Weinberg, R. A., 2009; Larue, L., & Bellacosa, A., 2005).

1.2.2 Tumor Hypoxia

The tumor microenvironment is a dynamic ecosystem due to diverse variables such as cell growth which can lead to nutrient depletion and the occlusion of blood vessels, all of which can contribute to fluctuations in oxygen availability (Albini, A., & Sporn, M. B., 2007; Detlev G. et al., 2006). Specifically, tumor's possess mechanisms that allow it to exist under varying oxygen levels. Hypoxia is experienced in tissues with an oxygen tension of 5% or lower, whereas normoxia is described as having an oxygen tension between 10-21% (Detlev G. et al., 2006). Hypoxia occurs when a tumor exceeds its blood supply and glucose consumption, resulting in oxidative stress that in turn alters the physiology of the tumor, and therefore, its gene expression as well (Brown, N. S., & Bicknell, R., 2001). It is important to note that hypoxia is not delimited to cancer, as it is seen in the other structures such as the bone marrow and the small intestine. However, its relevance in cancer physiology is due to the fact that the response genes essential for metabolic adaptation, in hypoxia, are strongly correlated with poor prognosis and tumor aggressiveness (Kim, Yuri et al., 2009; Tan, E. Y. et al., 2009).

HIF1-α, a subunit of the transcription factor HIF, plays a role in regulating glycolytic enzymes, angiogenesis, tumor invasiveness, and metastasis (Ilie, M. et al., 2013; Mirzoeva, S. et al., 2008; Ullah, M. S. et al., 2006). Additionally, HIF1-α mediates the export of lactic acid from the cell through MCT4, a transporter that couples lactate with a proton (Ullah, M. S. et al., 2006; Supuran, C. T., 2008). Lactate transport is an essential function in glycolytic tissue and especially in hypoxic microenvironments in order to ensure that glycolysis continues, and it has been shown that HIF1-α is directly involved in the development of cancer and apoptosis (Ullah,

M. S. et al., 2006; Minet, E. et al., 2000). There is increasing evidence that the transcription factor complex HIF-1α, typically stabilized under hypoxic conditions, is now being more frequently investigated under normoxic conditions due to its presence in a variety of cancers, though the PI3-kinase (PI3K) pathway and other uncharacterized pathways (Tan et al., 2004; Saramäki, O. R. et al., 2001). Moreover, there is also a lot of research indicating the intersection of HIF expression and EMT events through the direct binding of the twist promoter by HIF, that which up-regulates its transcription and translation (Yang, M.-H. et al., 2008). In fact, there is new evidence supporting HIF1-α's involvement in extra-cellular membrane (ECM) degradation and invasion in a variety of cancers in normoxia (Yang, M.-H. et al., 2008). Lastly, previous studies demonstrate HIF-1α promotes chemoresistance in prostate cancer under normoxic conditions (Saramäki, O. R. et al., 2001). Due to the extensive ties between both EMT and hypoxia and their suspected involvement in chemoresistance, it makes them interesting targets for interrogation.

1.3 Chemotherapy and chemoresistance

The medical history pertaining to the development of chemotherapy is very interesting; having first been discovered during WWII when scientists noticed that mustard agents depleted the white blood cell counts of soldiers (DeVita, V. T., & Chu, E., 2008). Today, chemotherapy is vital for treating a variety of cancers; its formulation depending on the stage, type, metastasis/receptor status, and previous cytotoxic exposure of a patient (Canadian Cancer Society, 2019). Clinically relevant drugs for BC treatment include: doxorubicin, docetaxel, gemcitabine, paclitaxel, and cisplatin (Canadian Cancer Society, 2019). Chemotherapy agents are

classified depending on their mechanism of action; for example, paclitaxel is a mitotic inhibitor that blocks microtubule depolymerization by binding the inner wall of β-tubulin, causing mitotic arrest (O'Reilly, E. A. et al., 2015; Zhang, J. et al., 2013). Alternatively, cisplatin is classified as a DNA alkylator and functions by reacting with purines, forming intra-strand crosslinks, subsequently kinking the DNA and interfering with DNA repair machinery, thereby inducing apoptosis (O'Reilly, E. A. et al., 2015; Horwitz, S. B., 1994).

Chemoresistance occurs when cancer cells maintain viability during cytotoxic therapy, and it may be innate or acquired, such that chemotherapy exposure and varying gene expression can lead to its development (Bosch, A. et al., 2010; O'Reilly, E. A. et al., 2015). This may be caused by a dysregulation of genes and variety of mechanisms including: efflux pumps, such as p-glycoprotein (MDR1) and MRP3 which prevents cytotoxicity in cells by removing the chemotherapy drug from the cytosol. Efflux pump expression may be inherent in a given cell-type or induced by the chemotherapy treatment (Modok, S et al., 2006). Mitotic checkpoint mutations result in the dysregulation of chromosome segregation during mitosis, frequently the result of chromosome instability, leading to events such as aneuploidy (Cahill, D. P et al., 1998). Enhanced DNA repair mechanisms are especially relevant, considering clinical therapies such as cisplatin function to damage DNA. In order for a cell to maintain genomic integrity, it must be able to repair the damage caused by cytotoxic agents, using a combination of homologous and non-homologous repair mechanisms (Rocha, C. R. R et al., 2018; O'Reilly, E. A. et al., 2015). Lastly, inhibitors of apoptosis (IAPs) are proteins that regulate caspase activity, metastasis, and cell invasion. This is due to a dysregulation of IAPs such as, cIAP1, cIAP2, and XIAP, resulting in resistance to apoptotic stimulation, making it vital for tumor survival (Gyrd-Hansen, M &

Meier, P., 2010). Research has established a significant amount of information concerning the mechanisms underlying chemoresistance, however despite this, treatment of TNBC remains a clinical challenge. Therefore, understanding how cells avoid apoptosis upon exposure to chemotherapy is of vital importance in order to better understand pre-existing and novel mechanisms propagating chemoresistance.

1.4 Apoptosis

Apoptosis, a cellular grim-reaper, drives programmed cell death in order to dispose of cells that are damaged, nonessential, or anomalous (Green, D. R., 2019; Sun, G. et al., 2017; Tang, H. M., & Tang, H. L., 2018; Lam, H. et al., 2011). Apoptosis originates from the Greek word "ἀπόπτωσις" meaning falling off, referencing the production of apoptotic bodies that separate from a fragmenting cell (Duque-Parra, J. E., 2005). Progression through the pathway leads to a series of events including, mitochondrial fragmentation, caspase activation and DNA damage, followed by cell death (Green, D. R., 2019; Sun, G. et al., 2017; Tang, H. M., & Tang, H. L., 2018; Lam, H. et al., 2011). Dysregulation of apoptosis can result in many diseases, including cancer, therefore homeostasis plays an important role even in the fine balance of death and survival-mediated pathways. Apoptosis plays a vital role in a variety of life stages, from as early as embryogenesis throughout the rest of our physiological life.

Phenotypic hallmarks of apoptosis are well-conserved and described in multi-cellular organisms, including cell shrinkage, membrane blebbing, apoptotic body formation, and chromatin condensation. Apoptosis can be broken down into early and late stages dependent on the

activation of different proteins, including the alleged delineation between the uncommitted and committed steps, which will be addressed later.

1.4.1 Intrinsic and extrinsic apoptotic pathway

Apoptosis can be activated through two distinct pathways dubbed “extrinsic” and “intrinsic” (Fig. 1.4). The activation of the extrinsic pathway relies on the stimulation of an extracellular death-receptor, TNF, leading to subsequent cascade initiation (Putcha, G. V. et al., 2002). While the activation of the intrinsic pathway results in the release of *cytochrome c* from the mitochondria after an apoptotic stimulus has been detected (Putcha, G. V. et al., 2002). In the end, both result in the cleavage and subsequent activation of caspases that lead to the terminal phase of apoptosis, death. It is also documented that on occasion there is communication between the two sub-pathways, where early products of the extrinsic pathway enhance mitochondrial membrane permeability (MOMP) leading to the eventual release of *cytochrome c* (Putcha, G. V. et al., 2002).

Prior to the activation of executioner caspases, pro-caspases must be cleaved and activated. This occurs through the binding of pro-caspase 9 to the APAF-1/cytochrome c complex (Végran, F. et al., 2011). Active caspase-9 is then able to recruit pro-caspase-3 resulting in its binding and subsequent activation, producing fragments p58 and p10 (Tang et al., 1998). Caspases are classified as cysteine-aspartate proteases, indicating a cysteine in the active site of the protease nucleophilically attacks the site directly following an aspartate residue in the target protein,

resulting in peptide bond cleavage. This results in the formation of the apoptosome, a heterodimer that results in the progression of end-stage apoptosis.

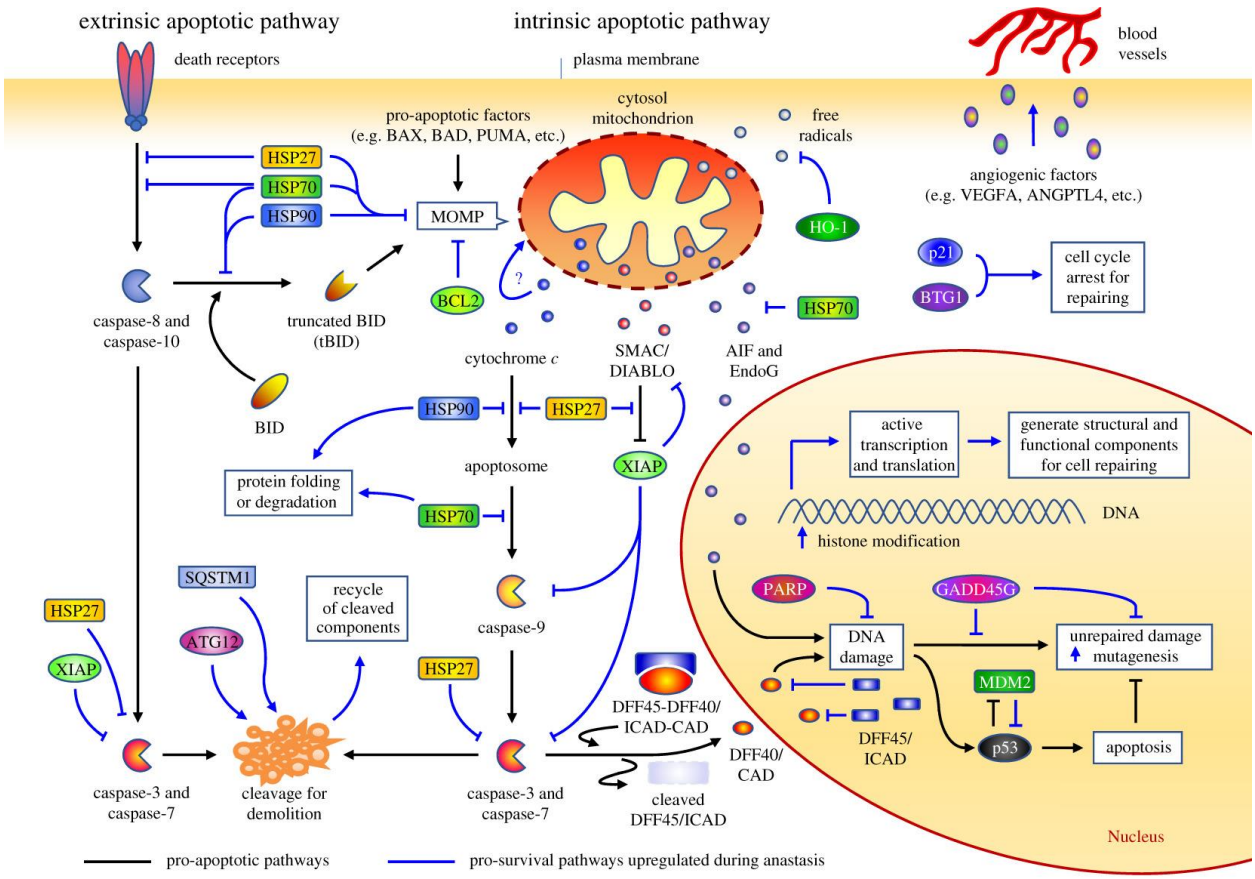

Fig. 1.4 Extrinsic and intrinsic activation of apoptosis in mammalian cells. Schematic depicting the complex molecular mechanisms through which apoptosis progresses, with their pro-survival counterparts depicted, all of which intersect at executioner caspase activation leading to cell death. Figure is modified from "Anastasis: recovery from the brink of cell death" (Tang, H. M., & Tang, H. L., 2018).

1.4.2 Role in the development of cancer and therapy

The dysregulation of apoptosis can have many dire effects on an organism's overall health, including but not limited to the development of cancer. Alterations can occur along many avenues in order to falter the pathway's finely tuned mechanism. This includes mutations in BCL2 family proteins, apoptosome defects, alterations in death receptor pathways, tumor suppressor inactivation, and changes in caspase activity (Favaloro, B. et al., 2012; Bedi, A. et al., 1995; Liu, K.-Q. et al., 2012). Additionally, an inability to activate apoptosis can not only lead to disease development, but also the acquisition of chemoresistance in an already established tumor. The link between the inhibition of apoptosis and deviations in executioner caspase levels is well-established, however, research has produced conflicting results. Both the increased and decreased presence of executioner pro-caspases is correlated with poor prognosis. A potential explanation for this discrepancy is the distinction between pro- and non-apoptotic activity of caspases and the isoform present (Hu, Q et al., 2014; Flanagan, L et al., 2016; Huang, H et al., 2010). Never less, it is clear that the inhibition of apoptosis serves a potential role in the acquisition and maintenance of chemoresistance, therefore, understanding the mechanism behind this inhibition must be investigated further.

1.5 Anastasis

It has long been believed that cells become committed to the apoptotic pathway once executioner caspases are activated, effectively sealing their fate (Lam, H. et al., 2011; Sun, G. et al., 2017b). However, in recent years this theory has been challenged by research showing that given the

opportunity, a subpopulation of cells are able to revert back to a pre-apoptotic state; in a new mechanism coined “anastasis”, originating from the Greek word “ανάσταση”, meaning “rising to life” (Lam, H. et al., 2011; Sun, G. et al., 2017b). As cells progress down the apoptotic pathway, they acquire additional genetic anomalies, leading to chromosome instability; however, when anastasis occurs, a small portion of these cells can survive and go on to function relatively normally, though there is increasing evidence that not all genetic aberrations are repaired (Tang, H. M., & Tang, H. L., 2018).

1.5.1 Potential role of anastasis in cancer development and chemotherapy treatment

As previously mentioned, anastasis results in the increased presence of newly acquired genetic aberrations or the dysregulation of signaling pathways through post-transcriptional mechanisms. It is possible that cancer cells having been exposed to chemotherapy could be inherently more resistant in comparison to those that have not undergone anastasis as a result (Lam, H. et al., 2011). Furthermore, this has the potential to shed some light on the observed increase in cancer risk in individuals with repeated tissue damage. Repetitive tissue damage, as seen in gastroesophageal reflux disease (GERD) for example, results in a higher incidence rate of esophageal cancer compared to those who do not suffer from the disorder. If these cells are in fact undergoing anastasis, this could be leading to the observed oncogenic transformation through the repeated interruption of apoptosis, suggesting that perhaps anastasis is carcinogenic (Lam, H. et al., 2011; Sun, G., & Montell, D. J., 2017a).

It is known that caspases can possess non-apoptotic roles and is observed frequently in human physiology during events such as, sperm maturation and neuronal dendritic remodeling (Ertürk, A. et al., 2014; Tang, H. M., & Tang, H. L., 2018; Sun, G., & Montell, D. J., 2017a). The major difference between apoptotic and non-apoptotic caspase-activation observed under normal conditions is the tight-regulation of caspase activity levels and its location within the cell, effectively limiting the cell's exposure. It has also been described to transpire in a time-dependent and regulated manner during discreet periods of an organisms' development, however how the cell is able to regulate the level of activity and its localization under these circumstances remains a mystery (Sun, G., & Montell, D. J., 2017a).

1.5.2 Transcriptomic signature of anastasis

Presently, there is very little research demonstrating the mechanism behind which anastasis propagates. However, Dr. Denise Montell's research has revealed that anastasis can be sub-divided into two stages: early and late stage anastasis. Changes in transcriptional signatures are evidence of this progression and demonstrate that anastasis is an active process, rather than a passive one (Sun, G., & Montell, D. J., 2017b). Interestingly, prior to the removal of an apoptotic stimulus, transcriptional upregulation of markers involved in cell proliferation, stress response, cell-cycle re-entry, and transcription are observed, allowing for translation of mRNA and rapid recovery once anastasis is initiated (Sun, G., & Montell, D. J., 2017b). One of the transcripts that is up-regulated and necessary for survival is Snail. As previously described, Snail plays a role in mediating EMT, and in addition to this, it has been shown to be protective against apoptosis (Wan et al., 2015). The above-mentioned study has shown that knocking-down Snail

significantly reduces the ability for cells to survive executioner caspase activation. In addition to this, late stage is demarked by the activation of genes involved in translation, the spliceosome, RNA transport, ribosome biogenesis, and protein processing, all of which indicate the re-initiation of translation (Sun, G., & Montell, D. J., 2017b).

Lastly, anastasis has been shown to be distinct from other cellular survival pathways, such as autophagy. While both contribute to cell survival, the transcriptional signature for the two pathways is distinct (Sun, G., & Montell, D. J., 2017b). In addition to these findings, while cells having undergone anastasis were shown to be more migratory, cells having initiated autophagy, in response to amino acid starvation, were not. Therefore, the molecular and behavioral markers of anastasis and autophagy are distinct.

1.5.3 Surviving caspases-3/7 activation

Anastasis is not delimited to cancerous cells, in fact, it has been observed in many cell types, ranging from cardiomyocytes to neuronal cells (Lam, H. et al., 2011; Tang, H. M., & Tang, H. L., 2018; Sun, G., & Montell, D. J., 2017b). As a result, it is believed this is an evolutionarily conserved phenomenon that serves the purpose of saving cells from death. However, why it would be better to save potentially damaged cells is not completely clear, though this certainly brings to light a new awareness of the homeostatic mechanism between life and death. There is speculation that this mechanism is important for safeguarding senescent cells, such as neurons in the central nervous system (CNS) and cardiomyocytes. Another point of contingency is that anastasis may drive stress-induced genetic diversification, allowing cells to survive in the

presence of what was originally an apoptotic stimulus. Lastly, cells may be able to regress from their apoptotic state due to the alleviation of cellular stress, which could be a result of cell death in nearby cells, increasing the concentration of available nutrients and other essential biomolecules in an otherwise deficient environment (Sun, G., & Montell, D. J., 2017a). This could also be due to the dynamic tumor landscape that results in changes to the microenvironment. This has been referred to as "developmental anastasis" and has been observed in different larval developmental stages of *Drosophila melanogaster* (Sun, G., & Montell, D. J., 2017a).

1.5.3.1 Detecting anastasis

Anastasis is difficult to detect as there are no established biomarkers for cells having gone through the process. At this moment in time the only way to distinguish cells that have undergone anastasis is to label cells for executioner caspase activation during apoptosis in order to observe a loss of activated caspase activity. The caspase 3 (Cas3) reporter used in this thesis utilizes a cyclized protein with a DEVDG polypeptide domain that is cleaved by DEVDases between amino acids D and G (Fig. 1.5). Once cleaved the protein complex can fold into a functional conformation, thereby expressing GFP as indicator of end-stage apoptosis initiation (Tang, H. M., & Tang, H. L., 2018). DEVDases are caspase-like proteases that cleave and activate executioner caspases, thereby allowing for the indirect quantification of cleaved caspases-3/7 in the cell (Tang, H. M., & Tang, H. L., 2018).

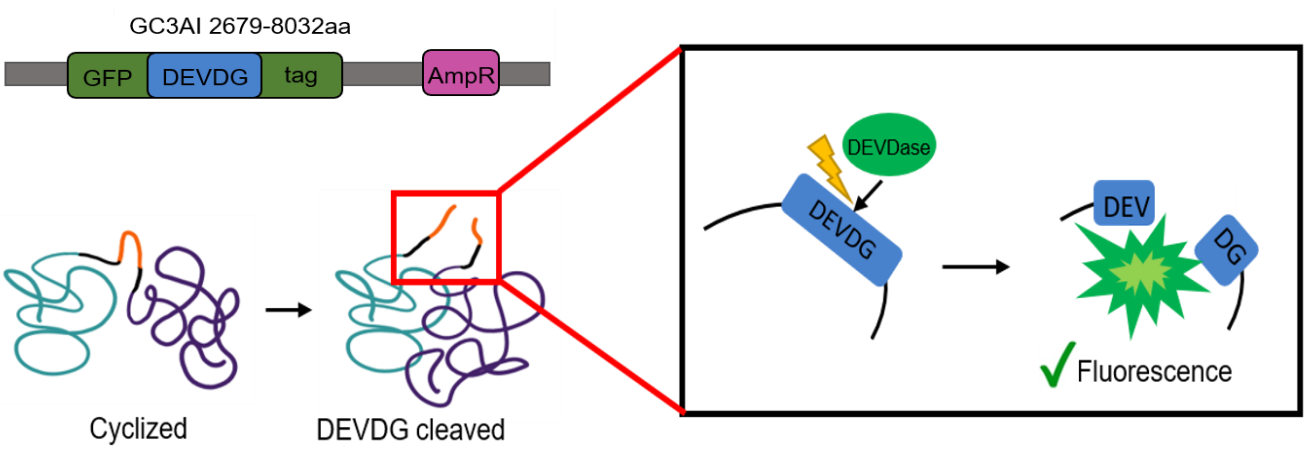

Fig. 1.5 GC3AI reporter indicates caspase-3 activation during end-stage apoptosis. Schematic depicting the mechanism of action through which DEVDases cleave and activate the GFP-tagged Cas3 reporter protein; depicting the cyclized GC3AI Cas3 reporter cleaved when DEVDases are present, allowing to take on its native conformation resulting in detectable fluorescence.

1.6 Hypothesis and Objectives

1.6.1 Hypothesis

By overcoming apoptosis, “Anastasis” contributes to tumor progression and drug resistance in triple-negative breast cancer.

1.6.2 Objectives

This thesis has two major objectives.

1.6.2.1 Determine a phenotype for chemotherapy-induced anastasis in TNBC

When this project began, previous studies concerning anastasis had been exclusively conducted on normal or cancerous cells induced to undergo apoptosis in the presence of ethanol or staurosporine (Lam, H. et al., 2011; Sun, G. et al., 2017). However, studies had yet to explore the effects of anastasis in cancer cells when exposed to clinically relevant chemotherapy drugs, such as paclitaxel and cisplatin. Therefore, I sought to establish the effects of anastasis on the phenotype of TNBC by generating BC cell lines that had undergone anastasis and comparing their molecular phenotype to their wild-type (WT) counterpart. The first objective of my thesis was to establish how anastasis affects a cell’s sensitivity to paclitaxel and cisplatin, the effect on cell invasion and migration, as well as metabolic activity. Lastly, I wanted to compare the growth kinetics, metastatic, and invasive propensity of these cells *in vivo*.

1.6.2.2 Determine a mechanism by which anastasis prevents apoptosis

While previous research has provided significant evidence supporting the existence of anastasis, there is very little known about the mechanism (Lam, H. et al., 2011; Sun, G. et al., 2017). The second objective of my thesis was to understand the molecular events that take place in the early stages of anastasis when a cell is recovering and how cells are capable of surviving lethal cas3 activation during end-stage apoptosis.

Chapter 2: Materials and Methods

2.1 Cell culture, antibodies, and reagents

The MDA-MB-231 and HEK293t human cell lines were obtained from the American Type Culture Collection (ATCC). The SUM159PT cells were provided by Dr. Sharon Gorski where they were originally obtained from BioIVT. The MDA-MB-231 and HEK293t cell lines were maintained in Dulbecco's modified Eagle's medium containing 25 mM glucose and 110 mg/L sodium pyruvate (Gibco cat # 11995-065, Burlington, Ontario, Canada) and supplemented with 10% fetal bovine serum (FBS; Gibco, Burlington, Ontario, Canada), while the SUM159PT cell line also required the addition of non-essential amino acids (1X NEAA), human insulin (5 µg/ml), and hydrocortisone (1 µg/ml). Cells were incubated in a humidified incubator at 37 °C with 5% CO_2. Cell lines were routinely tested for mycoplasma contamination using either the LookOut Mycoplasma PCR detection kit (Sigma-Aldrich, Oakville, ON, Canada; Cat. No. MP0035) or the MycoAlert Mycoplasma Detection kit (Lonza, Mississauga, ON, Canada). Additionally, cell lines used in the manuscript have been authenticated using short tandem repeat DNA profiling (DNA fingerprinting) by a commercial testing facility (Genetica, Burlington, NC, USA).

The mouse anti-ILK (Cat no. 611803), mouse anti-vimentin (Cat no. 550513) antibodies were obtained from BD Biosciences (Mississauga, Ontario, Canada). The monoclonal rabbit anti-SNAI1 (Cat no. C15D3), monoclonal rabbit anti-SNAI2 (Cat no. C19G7), monoclonal rabbit anti-cleaved-caspase-3 (Cat no. 9664S), rabbit anti-PARP (Cat no. 9542S), and monoclonal

rabbit anti-cleaved-PARP (asp214) (Cat no. 5625) were obtained from Cell Signalling Technology Inc (Danvers, MA, USA). The polyclonal (C-term) rabbit anti-HIF1α (Cat no. 10006421) antibody was obtained from Cayman Chemical Company (Ann Arbor, MI, USA). The polyclonal rabbit anti-caspase-3 (Cat no. 06-735) antibody was obtained from Upstate Biotechnology Inc – now EMD Millipore (Temecula, CA, USA). The monoclonal mouse anti-β-actin (Cat no. A5441) antibody was obtained from Sigma-Aldrich (St. Louis, MO, USA).

2.2 Generation of stable cell lines

2.2.1 Transduction of HEK293t with GC3AI packaged lentivirus

For the production of lentivirus containing the GC3AI plasmid, $2x10^4$ cells/cm^2 were plated in 6-well plates and were incubated for 24 h. Plasmid master mixture included CMV-dr8.91 packaging plasmid (0.9 µg/well), VSV-G/pMD2.G envelope plasmid (0.1 µg/well), lentiviral vector plasmid (1 µg/well), and OPTI-MEM (up to 125 uL), and was incubated at RT for 5 mins. Subsequently, TransIT-LT1 reagent was diluted in OPTI-MEM (1:20) and incubated at RT for 5 mins. The plasmid master mix was added dropwise to the TransIT-LT1 reagent, and then incubated for 30 mins. The mixture of reagents was added to HEK293t cells and incubate for 18h. Changed and replenished media and incubated for an additional 24h. Media containing virus was then harvested and filtered through a 0.45 µm syringe filter and stored at -80 °C for future use.

2.2.2 Transfection of TNBC lines with lentivirus GC3AI Cas3 reporter

Cells were seeded at densities of 1-2x10^5 cells in 6-well plates and incubated for 24 h. A ratio of 1:400 viral media was added to DMEM media and 1X polybrene. Add transduction mixture to cells and incubate for 24 h. Wash cells twice with 1X PBS, replenish growth media, and incubate for 48 h. Select cells using 3 ug/ml Puromycin (Cat no. P8833-100MG, Sigma Aldrich) for 72 h.

2.3 Cell viability

Cells were seeded at 1-2.5x10^3 cells per well in 96-well, black/clear tissue culture plates (Cat no. 655097, VWR) and allowed to attach overnight. Treated with increasing doses of cisplatin (100 nM – 50 uM) and paclitaxel (1 nM – 50 nM) and incubated for 72 h. Cell titer glo © (Cat no. G7572, Fisher Scientific/Promega) protocol previously described was used and luminescence was measured in the Spectramax i3 plate reader (Molecular Devices).

2.4 Flow cytometry

1x10^6 cells were trypsinized and resuspended in FACS buffer (PBS pH 7.4 +3% FBS). Cells were washed with cold PBS and then with 0.2 µm filtered 1X binding buffer (10X – 0.1 M Hepes, 1.4 M NaCl, and 25 mM $CaCl_2$), with the cells being centrifuged at 1200 rpm for 5 mins after each wash and the supernatant being aspirated each time. The pellet was incubated in 1:50 annexin-V antibody (Cat no. 640906, Cedarlane) for 10 mins at 4°C, then was resuspended in 500 µl of FACS buffer containing 1:10,000 propidium iodide (Sigma-Aldrich, P4170). A

minimum of 10,000 events were collected per sample using the BD LSR Fortessa II (BD Biosciences, Mississauga, Ontario, Canada), and analyzed using the software FlowJo (FlowJo LLC, Ashland, OR, USA). Gating for annexin-V signal was placed between the two cell populations, at a signal fold-change of $10^3 – 10^4$, consisting of negative and positive-annexin cells, respectively.

2.4.1 FACS – fluorescence activated cell sorting

$1x10^7$ cells were trypsinized and suspended in FACS buffer (PBS pH 7.4 +3% FBS) and washed in cold PBS twice, centrifuged at 1200 rpm for 5 mins after each wash, where the supernatant was aspirated. The pellet was then resuspended in 1 mL of FACS buffer treated with 1:10,000 propidium iodide (Sigma-Aldrich, P4170) and stored on ice while not sorting. Sorting was performed on the FACSAria III (BD Biosciences, Mississauga, Ontario, Canada), into 5 mL FACS collection tubes that contained 2 mL of 1:1 media and FBS. Gating for positive cas3 signal was placed between the two cell populations, at a signal fold-change of $10^3 – 10^4$, consisting of negative and positive-GFP cells, respectively. Approximately, $3.4x10^4$ cells were collected per sample and subsequently centrifuged at 1200 rpm for 5 mins and resuspended in 100 µl of 1:1 ratio of media to FBS and pipetted into a single well in a 96-well clear plate (VWR) and incubated, with frequent media changes. $2x10^4$ events were collected per sample, and were analyzed using the software FlowJo (FlowJo LLC, Ashland, OR, USA).

2.5 Protein expression analysis

Cells were grown, in the above-mentioned incubation conditions, for 24 – 72 h to compare EMT marker expression levels in both parental and post-anastatic cells under conditions that include, untreated and treated with chemotherapy, followed by lysis at 4 °C in RIPA (50 mM Tris, pH 7.5, 150 mM NaCl, 1% NP-40, 0.1% SDS and 0.5% NaDoc). Equal amounts of lysate (5-80 μg) were loaded onto SDS–PAGE gels. Western blots were performed as described previously (65), with the addition of briefly fixing the membrane in MeOH and allowing to air dry before incubating with primary antibodies, using mouse anti-ILK (1:10,000), mouse anti-vimentin (1:5000), rabbit anti-SNAI1 (1:500), rabbit anti-SNAI2 (1:500), rabbit anti-HIF1α (1:1000), mouse anti-Twist1 (1:100), rabbit anti-caspase-3 (1:500), rabbit anti-cleaved-caspase-3 (1:500), mouse anti-cytochrome-c (1:300), rabbit anti-PARP (1:500), rabbit anti-cleaved-PARP (asp214) (1:500), and mouse anti-β-actin (1:10 000) primary antibodies. All secondary antibodies were used at 1:5000.

2.6 Time-lapse imaging (immunofluorescence)

Cells were cultured in 8-well chamber ibiTreat μ-slides (ibidi) overnight in order to reach 50% confluency, then treated with cisplatin (12 μM) or paclitaxel (15 nM) and incubated for 18 – 24 h. Cells were then washed twice with 1X PBS and replaced with fresh media (supplementation previously described). Cells were imaged at a magnification of 20X using a Colibri microscope (Zeiss) imaging with an Axiocam MRC at 30 mins intervals in an incubation chamber at 37^{o}C and 5% CO_2 and were processed using Photoshop CS5.1 (v12.1).

2.7 Quantitative real-time PCR

Whole cell extracts were processed using the RNeasy mini kit (Cat no. 74104, Qiagen) and stored at -80°C. cDNA was synthesized from RNA samples using the Iscript Advanced cDNA synthesis kit for RT-qPCR (Cat no. 172-5037, Biorad) with a program on the T100 thermal cycler (BioRad) of 20 mins at 46°C and 1 min at 95°C. 1µg of cDNA was pipetted into each well of a 384-well MicroAMP® Optical Reaction Plate (Cat. 4309849, Thermo Fisher), along with TaqMan fast advanced master mix (Cat no. 4444557, Thermo Fisher) and Taqman gene expression assays (FAM) for the following human targets (Cat no. 4331182, Thermo Fisher): Vimentin (Assay ID. Hs00958111_m1), ILK (Assay ID. Hs01101168_g1), SNAI1 (Assay ID. Hs00195591_m1), SNAI2 (Assay ID. Hs00161904_m1), Twist1 (Assay ID. Hs01675818_s1), HIF1α (Assay ID. Hs00153153_m1), GAPDH (Assay ID. Hs03929097_g1). Fast SYBR green master mix was used alongside the PrimePCR SYBR Green Assay: human GAPDH (Cat no. 10025716, Biorad) and primer sequences of the caspase-3 locus (Thermofisher), amplified using forward 5'-CTGGACTGTGGCATTGAGACA-3' and reverse 5'-AGTCGGCCTCCACTG-GTATTT-3', and caspase-3s was amplified using forward 5'-AGAAGTCTAACTGGAAAACCCAA-ACT-3' and reverse 5'-CAAAGCGACTGGATGAACCA-3' (28). MicroAMP® optical adhesive film covered the wells and the assay was performed using a Quant Studio 6 Thermocycler (Applied Biosystems). Data was analyzed in GraphPad Prism v.8.0.

2.8 Comet assay

Performed using the CometAssay Kit© (Cat no. 4250-050-K, Trevigen). Slides were imaged at 20X magnification, using a Colibri microscope (Zeiss) imaging with an Axiocam MRC. Data was analyzed using a plug-in, developed by the Sterling lab, in ImageJ (v1.45s, National Institutes of Health, Bethesda, MD, USA).

2.9 Wound-induced migration and invasion assays

A scratch-wound migration assay was performed using the Incucyte™ live cell analysis instrument (Essen Biosciences). SUM159PT cells were plated (30,000 cells/well) in order to form a monolayer in a 96-well Imagelock™ plate (Cat no. 4379, Essen Biosciences) and incubated for 24 h. Proliferation of the cells was inhibited with 5 µg/ml Mitomycin C (Cat no. M4287, Sigma) for 2 hours prior to making a wound in the monolayer. A Woundmaker™ tool, consisting of 96-pins was used to create a uniform wound in every well. The wound was imaged in brightfield every 2 h for a period of 24 h, with a Nikon Plan Fluor 10x/0.3 NA objective. Migration was quantified as the percentage of wound filled in by the cells over the indicated period of time.

Cells were incubated in serum-free media for 24 h, subsequently trypsinized and seeded into Corning © BioCoat™ Growth Factor Reduced Matrigel Invasion Chambers with an 8.0 µm PET membrane (Cat no. 354483, VWR). Media with 10% FBS and 100 ng/mL rEGF (Sigma-Aldrich) was used as a chemoattractant. The cells were allowed to invade for a period of 18 h, after which

the cells that had not invaded were carefully removed with a cotton-swab, taking care not to touch the bottom side of the well. The invaded cells on the bottom of the well were carefully fixed in 4% paraformalin in PBS, washed with dH_2O, and then stained with Hoescht 33342 (2 μg/mL) for 10 mins. The stained wells were placed upon a glass slide with a small volume of dH_2O and were imaged in approximately 5 fields at 10X magnification, using a Colibri microscope (Zeiss) imaging with an Axiocam MRC.

2.10 Mouse tumor models

All animal studies and procedures were performed in accordance with protocols approved by the Institutional Animal Care Committee at the BC Cancer Research Centre and University of British Columbia (Vancouver, BC, Canada). SUM159PT and/or SUM159PT/AC tumor cell lines were inoculated into 14-week old female NSG (NOD.CB17-Prkdcscid/J-IL-2R-/-). Cells were injected subcutaneously into the 4^{th} mammary fat-pad. Mice were allocated to different groups based on the cell lines that were injected, and the investigators were not blinded.

2.10.1 Growth kinetics

The sample size (n=10) per cell line, with n=8 going to end-point and n=2 harvested at 100 mm^3. No mice were excluded during the course of the study. Tumor sizes were determined via caliper, mice were weighed, and clinical observations performed three times per week. Bisected tumors and metastases were embedded for future IHC experimentation while the other half of the tumors were flash frozen in liquid nitrogen and stored at -80^oC for future western blot analysis.

2.11 Metabolic extracellular flux assay

2.11.1 Glycolysis stress test

Glycolytic activity was assessed using the glycolysis stress test kit (Cat no. 103200-100, Agilent) in a Seahorse X96F Analyzer (Seahorse Bioscience, Agilent). Cells were seeded (5000/well) in an XFe96 assay plate (Cat no. 101085-004, Agilent) and incubated overnight. During the course of the experiment cells were exposed to 1 µM oligomycin, 10 mM glucose, and 100 mM 2-DG. Capture of data was completed using the software Wave (Agilent), and was normalized to cell number using CellTiter Glo © (Cat no. G7572, Fisher Scientific/Promega), previously described, and analyzed using GraphPad Prism v8.0.

2.12 Statistical analysis

Statistical analyses were performed using GraphPad Prism v7.0 and v8.0. For comparison of two data sets containing three or more replicates, a two-tailed, unpaired Student's t-test with Welch's correction for unequal variances was performed. Statistical significance was set at $p \leq 0.05$.

Chapter 3: The role of anastasis in chemoresistance and metastasis

3.1 Tracking anastasis using the Cas3 reporter system

Anastasis has been previously identified in a variety of cell types, although its effects have never been tested in cancer cells when using clinically relevant chemotherapy drugs as an apoptotic stimulus. In order to identify and enrich for tumor cells that have undergone anastasis after exposure to chemotherapy drugs, I established a protocol that would allow the collection of cells poised for anastasis. To accomplish this, GC3AI, a cas3 reporter, was used to identify cells that were in the end-stages of apoptotic cell death (Zhang, J. et al., 2013). The cas3 reporter is a cyclized protein with the peptide region DEVDG that is recognized and cleaved by DEVDases, a protease that activates executioner caspase-3/7 (Fig. 1.5). Once this peptide sequence is cleaved, the protein may take on its functional conformation, allowing it to fluoresce green due to the presence of a GFP tag. The level of GFP is therefore proportional to the levels of DEVDases and consequently that of active cas3 in real-time in the cell (Zhang, J. et al., 2013). Therefore, the process of anastasis was demarked by the disappearance of the GFP signal and the subsequent return to a viable phenotype. This reporter allowed us to determine the exact moment a cell was undergoing anastasis, in order to study its effect on the cancer cell's response to chemotherapy treatment. Apoptosis was initially detected by measuring annexin-V binding to phosphatidylserine on the extracellular side of the plasma membrane (Fig. 3.1). Annexin-V was used to determine the appropriate chemotherapy dose for the cells in order to induce apoptosis. However, for sorting experiments the cas3 reporter was a much better indicator of anastasis, as annexin-V does not confidently indicate late-stage apoptosis. The dose was chosen based on a set

of flow cytometry experiments to observe the number of cells that entered apoptosis after overnight treatment (Fig. 3.2). The dose that created the greatest increase in cell number while limiting the drug exposure was selected. With reference to cisplatin, the doses of 10 µM, 20 µM, and 50 µM were interrogated. The percentage of viable cells increased from 0.07% to 0.21% between 10 and 20 µM, with no significant change at 50 µM. Therefore, a series of treatments between 10-20 µM were performed and 12 µM was selected. The exact same experiment was performed in order to determine the concentration of paclitaxel (15 nM).

The caveat when comparing chemotherapy dose given to a patient in a clinical setting versus to cells *in vitro,* is the target availability of the drug. Chemotherapy accessibility *in vitro* is not a concern, however, in patients, tumor characteristics and drug type can alter the efficacy of drug delivery to the tumor. This is due to the rate of drug clearance, which varies between patients, and the physical barriers of solid tumors, including: vascularization and blood flow, lymphatic fluid transport and drainage, interstitial space accessibility, and tissue "stiffness", the amount of collagen, of the extracellular matrix (Hoon, J et al., 1985). Conventional cisplatin concentration dose can range from 100-120 mg/m^2 per week with the highest dose being 200 mg/m^2 before nephrotoxicity becomes a concern. Paclitaxel can be safely tolerated at 100 mg/m^2 per week (Corden, B. J et al., 1985; Kelly, W et al., 2001). Based on a 10 cm tissue culture plate, used during this study, with a surface area of 0.0055 m^2, clinically relevant doses of cisplatin and paclitaxel would be 183 µM and 64 µM, respectively. Therefore, the dose administered to these cells is far below what is provided in a clinical setting, however, this does not consider the above-mentioned obstacles of drug availability.

Next, the cas3 reporter was stably expressed in human TNBC cells by producing reporter-containing lentivirus particles in HEK293t packaging cells (transfection), with the subsequent infection of SUM159PT and MDA-MB-231 cells with the lentivirus (transduction). The cells were then selected using 3 µg/ul of puromycin, a concentration that was previously determined by performing a kill-curve on the cells. FACS and immune-fluorescence (IF) imaging demonstrated basal fluorescence in the cells, that when treated with paclitaxel or cisplatin, exhibited a 10-fold increase of the GFP signal. In order to select for cells undergoing anastasis, SUM159PT-Cas3 cells were cultured and treated with either paclitaxel or cisplatin for 18-24 h, in order to induce executioner caspase activation, after which the chemotherapy agent was removed (Fig. 3.3, 3.4 ii). The treatment incubation was chosen in order to maintain a living population. After the 18-24 h treatment, cells were sorted using propidium-iodide (PI) (10 µg/mL), in order to distinguish living and dead populations, collected, and cultured in fresh media with increased concentration of FBS until they began to proliferate normally (Fig. 3.4 ii). Cells that were sorted and underwent anastasis were then imaged and did not possess any observable phenotypic variances when compared to the parental cell line from which they were developed (Fig. 3.4 i & iii). Together, these results support the ability for cells to not only undergo anastasis but function and proliferate normally in the following weeks and months activation of executioner caspases.

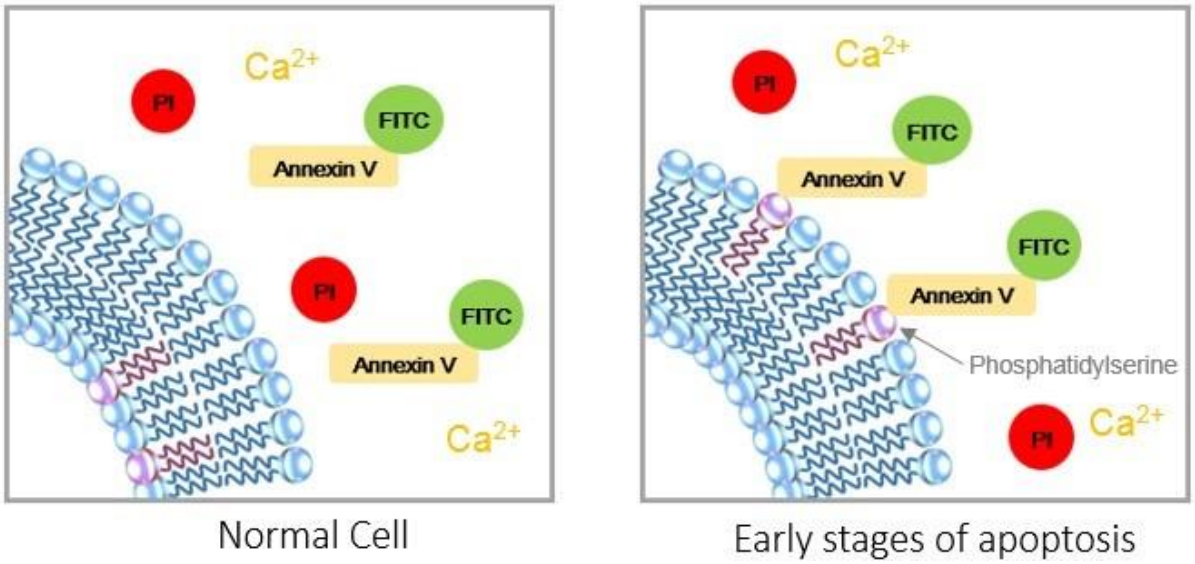

Figure 3.1 Annexin-V binds phosphatidylserine on the extracellular surface of the plasma membrane during early-apoptosis in the presence of a Ca^{2+}. A schematic depicting the display of phosphatidylserine on the ECM during the early-stages of apoptosis. Annexin-V functionalized with FITC can then bind allowing for its detection during a flow cytometry experiment. FITC has an excitation maximum of 490 nm and an emission maximum of 525 nm. Figure adapted from Dojindo's Annexin-V, apoptosis detection kit (Dojindo, 2019).

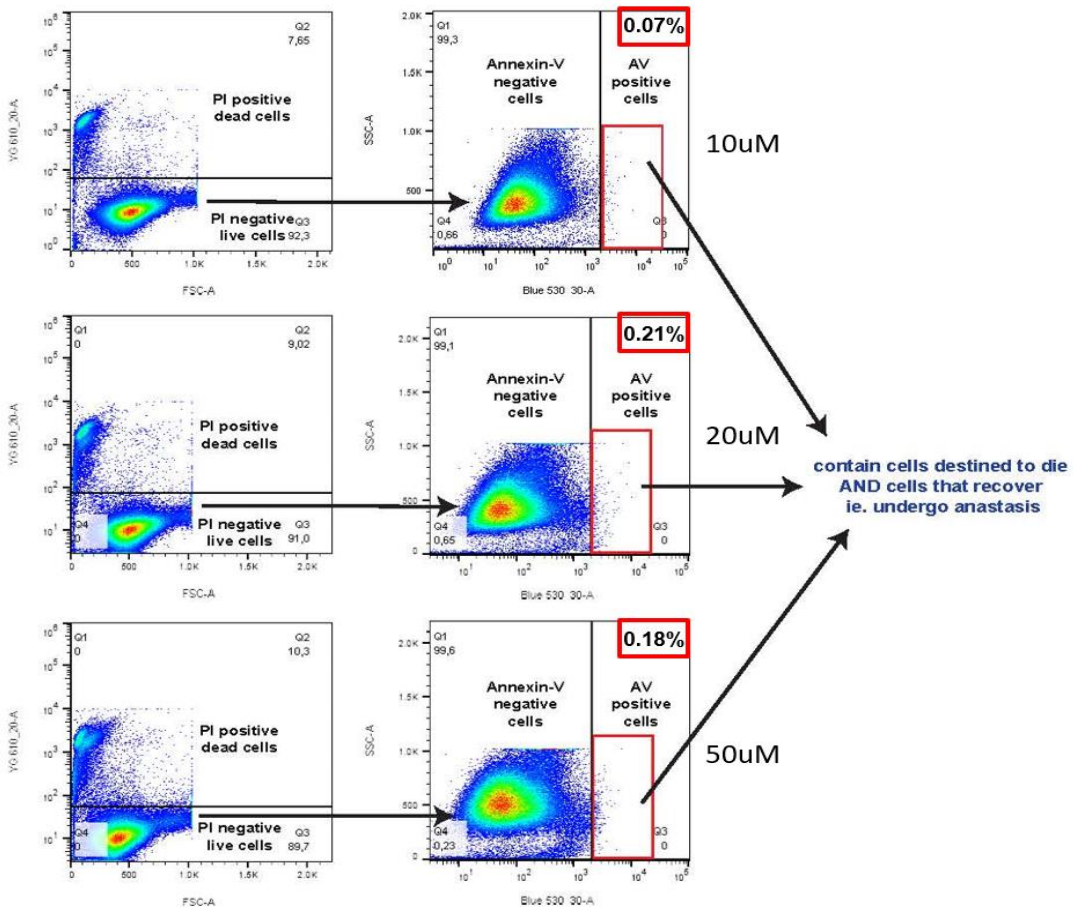

Fig. 3.2 Determining cisplatin concentration for inducing anastasis in SUM159PT cells using annexin-V as an indicator for early-stage apoptosis. Schematic depicting three FACS derived graphs *(top, middle, and bottom)* with SUM159PT cells treated with 10 µM (*top panels*), 20 µM (*middle panels*), and 50 µM (*bottom panels*) of cisplatin. Annexin-V was quantified only in viable PI-negative cells. The greatest percentage of gated (10^3 – 10^4 (Blue 530 – FITC signal)) viable cells with a positive annexin-V signal was determined to be between 10 – 20 µM as described in the methods.

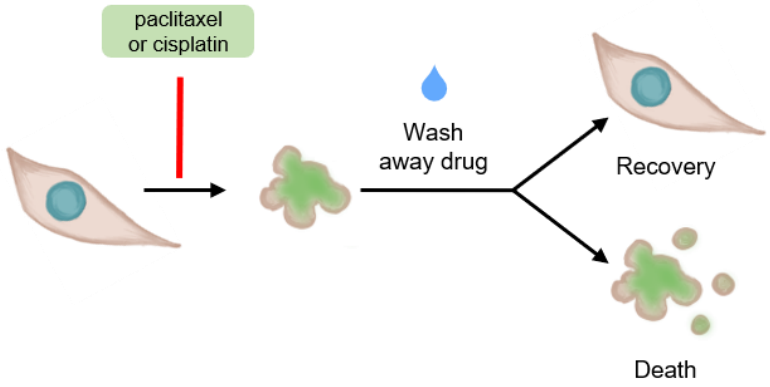

Figure 3.3 Induction of anastasis in stably expressed Cas3 reporter cells lines. Schematic depicting the stepwise induction of anastasis through the treatment and removal of paclitaxel and cisplatin as described in the methods. GFP-positive cells indicate the presence of active caspase-3 during end-stage apoptosis.

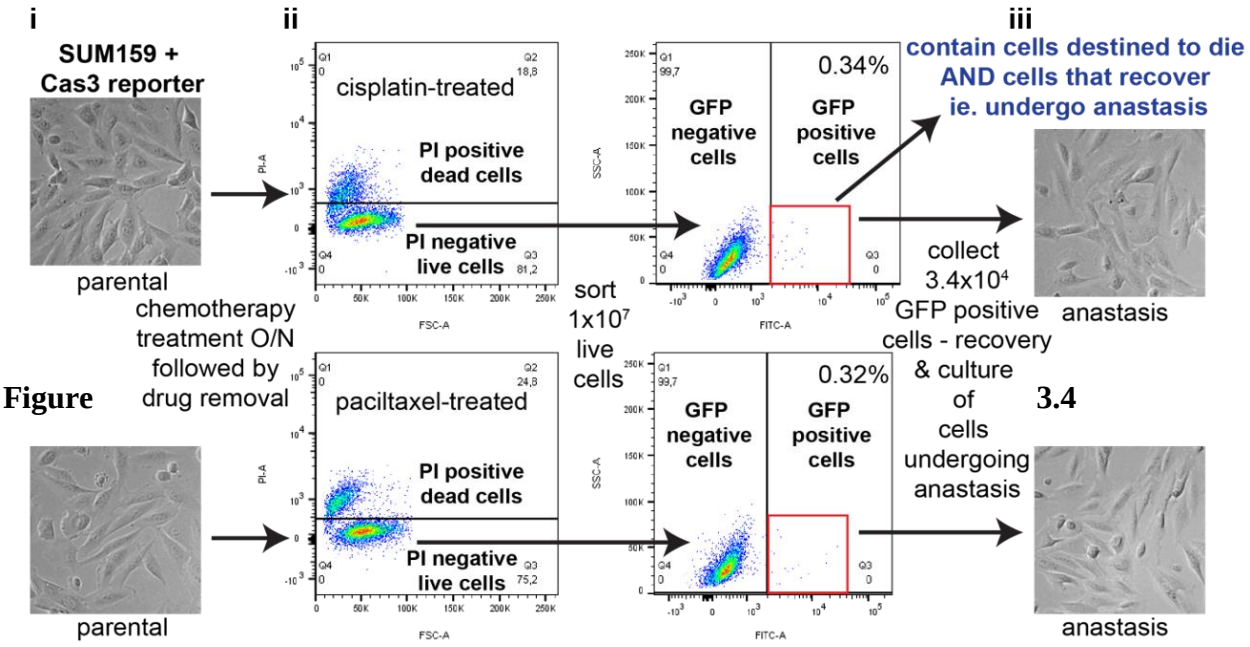

Figure 3.4 Identification and collection of apoptotic cells using a GFP-tagged Cas3 reporter for fluorescence activated cell sorting. i. Images showing then parental SUM159PT-Cas3 cell line prior to overnight treatment, with either paclitaxel or cisplatin, and FACS sorting. ii. FACS diagram depicting the gating (10^3 – 10^4 signal fold-change), as described in the methods, of varying signals (GFP and PI) captured from the SUM159PT-Cas3 cells treated for 18-24 h with either paclitaxel (15 nM) or cisplatin (12 μM). PI-negative, GFP-positive cells were collected during FACS sorting and plated in fresh media with an increased concentration of FBS. iii. Images showing post-anastatic SUM159PT-Cas3 cells that have recovered from end-stage apoptosis, with no observable phenotypic difference to the parental line prior to sorting.

In addition to the above results, I was interested in observing the morphological changes of cells undergoing apoptosis and anastasis in real-time, using IF colibri microscopy. Cells were cultured on microscope compatible chamber slides, treated and then washed, as described above (Fig. 3.3). SUM159PT-Cas3 and MDA-MB-231-Cas3 cells were imaged at 30 mins intervals for a minimum of 8 h, after washing away the chemotherapy agent, in order to observe anastasis taking place (Fig. 3.5) as described for HeLa cells exposed to ethanol by Sun, G. et al., 2017. During the period of imaging, cells were placed at 37^{o}C and 5% CO_2 to ensure optimal conditions under which they normally grow in an incubator. GFP-positive apoptotic cells were monitored in real-time and as time progressed one of two events were observed; the cell began to re-adhere to the substrate, while the fluorescence disappeared, indicating a loss of cas3 activity, while once again displaying a normal phenotype (Fig. 3.5 A, B, C (*arrows*)). On the other hand, if the cell did not recover, it continued down the apoptotic pathway, presenting well described hallmarks of apoptosis, including membrane blebbing and the production of apoptotic bodies (Figure 3.5 A, B, C (*arrow heads*)) (Tomei, L.D. & Cope, F.O., 1991). It is important to note that the apoptotic cells in some cases would lose their fluorescence simply due to the fact that the cell would rupture or break into smaller apoptotic bodies. Therefore, the disappearance of the fluorescence, must be observed in tandem with a normal morphological phenotype in order to show anastasis has occurred.

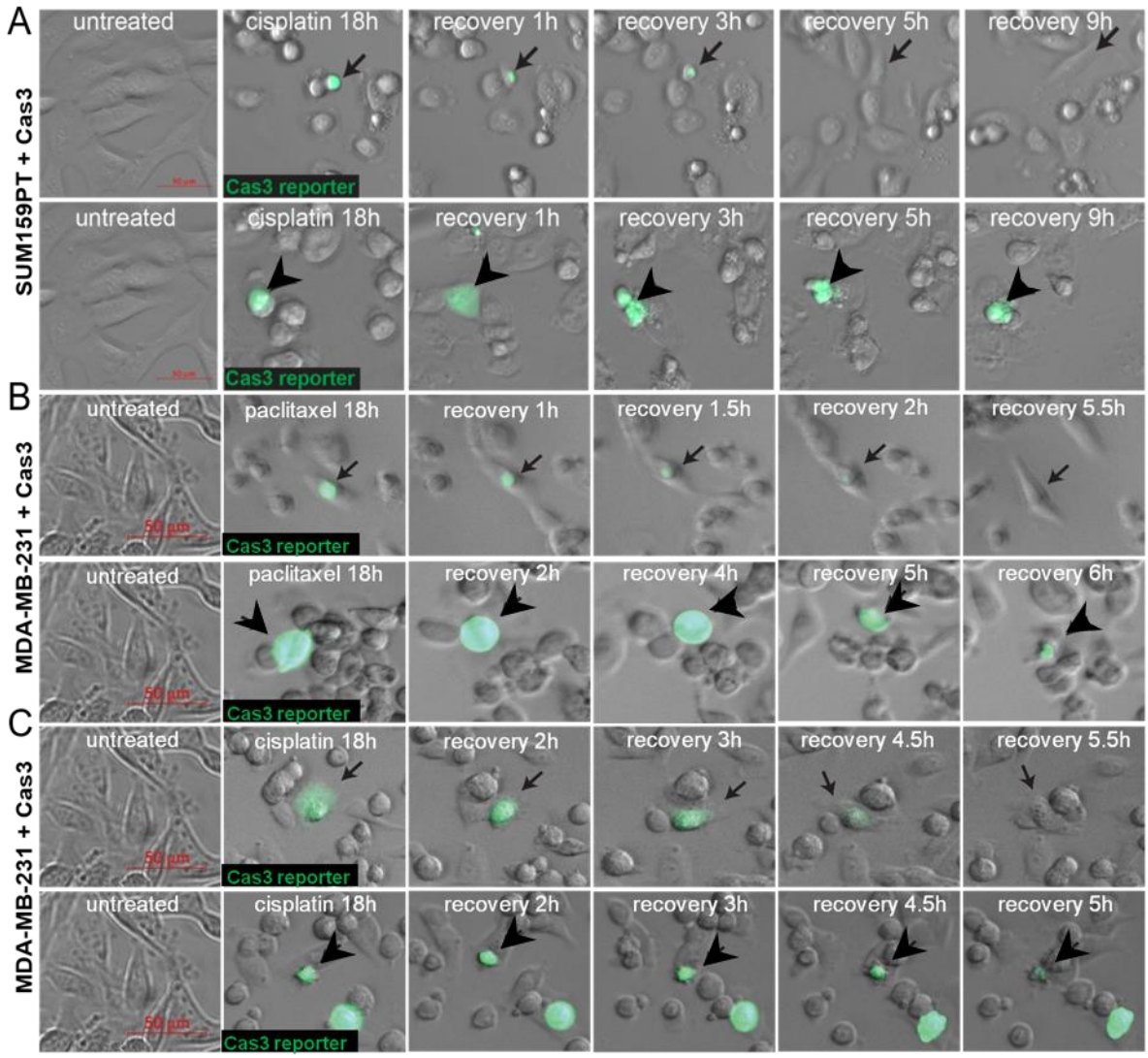

Figure 3.5 A cas3 reporter demonstrates a small number of cells are capable of surviving end-stage apoptosis after the removal of chemotherapy and returning to a normal phenotypic state. (A) Images of untreated and treated SUM159PT-Cas3 cells. Cells were treated for 18 h before being washed and replenished with untreated media. Cells treated with 12 µM cisplatin. Top panels depict a round, green cell that over time lays down flat and loses its fluorescence. Bottom panels depict a round, green cell that overtime does not recover and shows hallmark signs of apoptosis, such as membrane blebbing. Scale bar, 50 µm. (B-C) Images of untreated and treated MDA-MB-231-Cas3 cells. Cells were treated for 18 h before being washed and replenished with untreated media. (B) Cells treated with 100 µM cisplatin. Top panels depict a fluorescent cell that is spread out, and overtime begins to migrate as the fluorescence disappears completely. Bottom panels demonstrates a small round, green cell that appears to be blebbing and producing apoptotic bodies as time passes. It does not recover. (C) Cells treated with 25 nM paclitaxel. Top panels depict a cell with fluorescence contained in the nucleus, that disappears as time goes and while the cell begins to spread out onto the substrate regaining a

normal phenotype. Bottom panels show a very fluorescent, round cell that continues to shrink as time goes on and it does not recover.

3.2 Anastasis contributes to chemotherapy resistance

Having successfully enriched for SUM159PT-Cas3 cells that had undergone anastasis through the FACS collection of GFP-positive and PI-negative cells, I next wanted to determine if post anastatic cells varied phenotypically, including whether there was any different in drug sensitivity between the post-anastatic and parental SUM159PT cells. Cells were cultured and treated with a dose-range of paclitaxel or cisplatin for 72 h, in order to assess the cell's IC_{50} post-anastasis. I observed a 2-fold increase in the IC_{50} when compared to the parental line treated with cisplatin, suggesting that anastasis may play a role in the development of acquired chemoresistance (Fig. 3.6A). In order to ensure the acquired resistance was not due to the presence of efflux pumps, multi-drug resistance protein-1 (MDR1) was interrogated and not found to be up-regulated in post-anastatic cells (Fig. 3.6 D-E). Lastly, a comet assay was performed in order to identify potential changes in DNA damage, looking specifically at double-stranded and single-stranded DNA breaks. It was expected that the parental cells would already possess a basal level of DNA damage, due to their malignant nature. Cisplatin-induced post-anastatic cells showed a significant increase in double-stranded DNA breaks, but not single-stranded breaks (Fig. 3.6B, Fig. 3.6C, Fig. 3.6 G). This data considered the %tail DNA in the comet tail, as this is a more reliable indication of DNA damage between data set replicates (Fig. 3.6 F).

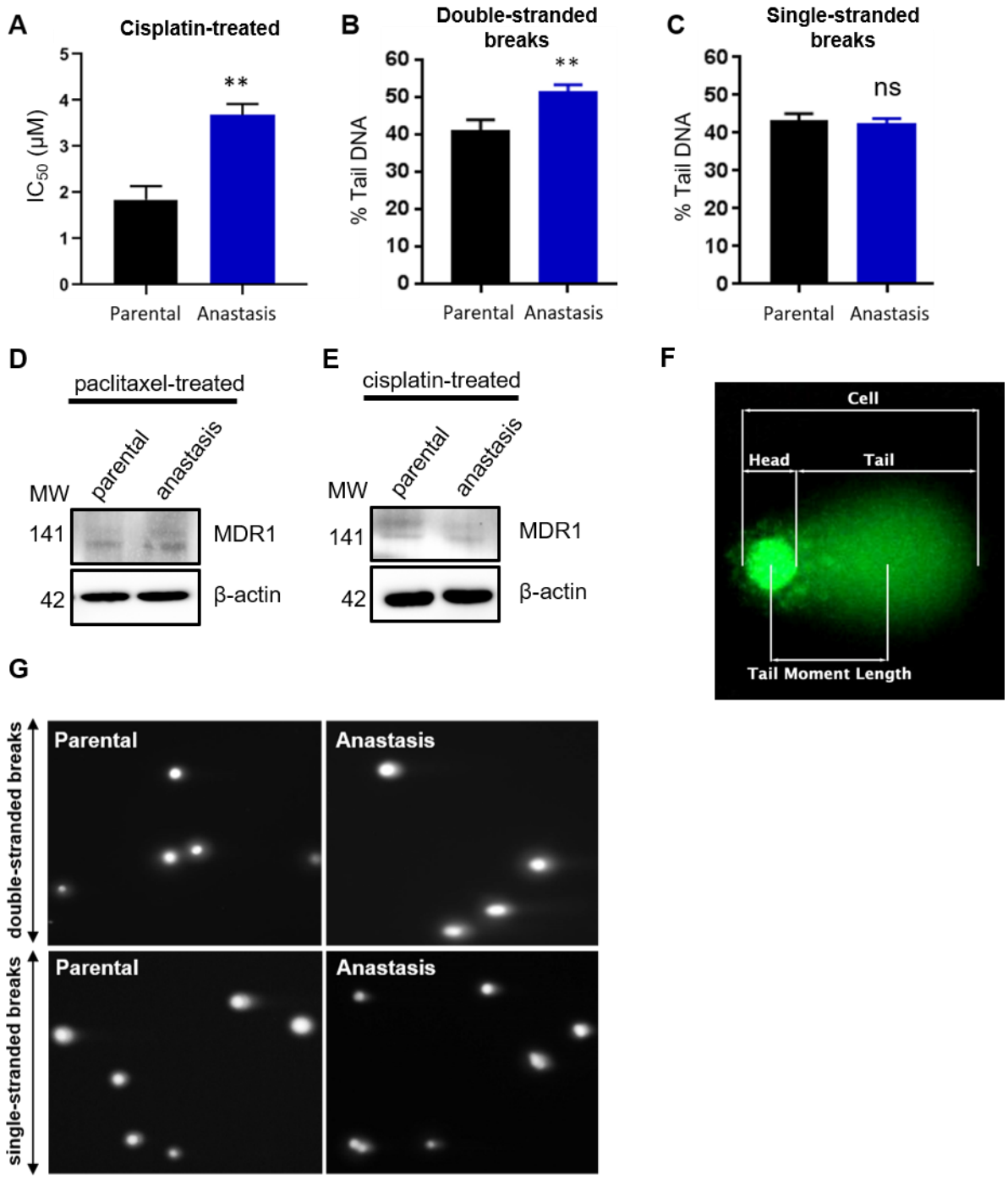

Fig. 3.6 Cells having undergone anastasis acquire resistance to cisplatin while exhibiting an increase in double-stranded DNA breaks but not single-stranded breaks (A) Assessing the viability of the parental and anastasis cell line upon exposure to cisplatin (500 nM – 50 uM). Data shows the mean ± s.e.m. of technical replicates (n=4/cisplatin concentration) and are representative of three separate experiments. **p≤0.01. (B) Comet assay analysis shows an increase in double-strand DNA breaks in cells having undergone anastasis. Data shows the mean

± s.e.m. of technical replicates (n=60/group) and are representative of three separate experiments. **p≤0.01. (C) Comet assay analysis shows no difference in single-stranded DNA breaks between the parental and anastasis cell lines. Data shows the mean ± s.e.m. of technical replicates (n=60/group) and are representative of three separate experiments. (D-E) Western blot analysis of drug efflux pump MDR1 in WT and post-anastatic SUM159PT cells. (D) Paclitaxel-treated (E) Cisplatin-treated (F) Diagram depicting the structural analysis of comets in a comet assay. % tail DNA is calculated through the integrated tail intensity multiplies by 100 and then divided by the total integrated cell intensity for a normalized measure of the percent of total cell DNA found in the tail (G) Images depicting comet assay where % tail DNA was determined using an ImageJ plug-in provided by the Peter Stirling lab. Comet head shown as a bright white circle, with the comet tail to the right in a smearing pattern, representing the DNA breaks.

3.2.1 Modulation of EMT and hypoxic stress responses

Having established that chemotherapy-induced anastasis does in fact incur resistance, I sought to gain further insight into the mechanism by which anastasis promotes this. EMT has been extensively studied in cancer, especially concerning its involvement in tumor progression and metastasis, and the development of chemoresistance in some cases (Tam, P. P. L. & Behringer, R. R., 1997; Yang, J., & Weinberg, R. A., 2008; Kalluri, R., & Weinberg, R. A., 2009; Timmerman, L. A. et al., 2004; Fischer, Kari R. et al. 2015; Kokkinos, M. I. et al., 2007). In fact, 90% of metastatic cases of TNBC tend to be resistant to treatment, making it a suitable target to explore (Bosch, A. et al., 2010; Cheng, G. Z. et al., 2007). Moreover, a previous study performed a global RNA screen on cells in the early stages of anastasis and observed the presence of snail in stress-granules (Sun, G. et al., 2017). Therefore, I sought to determine if EMT associated markers were involved in the aftermath effects of anastasis-induced chemoresistance. Indeed, through western blot and qPCR analysis, EMT markers including slug (SNAI2), snail (SNAI1), and Twist-1, were found to be significantly up-regulated in both cisplatin and paclitaxel treated post-anastatic SUM159PT-Cas3 lines (Fig. 3.7 A-D). Due to a subset of clinical TNBC cases

resembling the molecular and histological phenotype of mesenchymal cells, decreased expression of e-cadherin and increased expression of vimentin, these results were intriguing (Jeong, H et al 2012). One of the proteins that has been shown to regulate EMT is the focal adhesion protein ILK. While changes in mRNA and protein levels of ILK were not as consistent as the other transcription factors, I wanted to interrogate if ILK kinase activity was altered in the post-anastatic cells. Indeed, the kinase activity of ILK was found to be up-regulated in cisplatin induced post-anastatic cells, while the mRNA levels increased in paclitaxel-induced post-anastatic cells (SUM159PT/AP) (Fig. 3.7 E). Due to the increase in activity and downstream markers, I questioned whether the use of an ILK inhibitor (QLT-0267) would have an impact on re-sensitizing the cells to the original chemotherapy treatment. It was observed that when SUM159PT/AC cells were treated with QLT-0267, they became re-sensitized to the original chemotherapy treatment (Fig. 3.8 A-B). However, QLT-0267 did not significantly affect the parental cell's response to the drug (Fig. 3.8 A & C). These findings suggest that EMT may play a role in chemoresistance driven anastasis, however this must be further investigated.

Research that has been previously described by the Dedhar lab demonstrates that the overexpression of ILK results in an up-regulation of HIF-1α in normoxia through the PI3-kinase (PI3K)/mTOR pathway in prostate cancer cells (Fig. 3.9) (Tan et al., 2004). Other studies have also recently demonstrated the connection between HIF-1α and PI3K pathway through Y-box binding protein-1 (YB1), an RNA-binding protein, in *KRAS* mutated breast cancer (Lefort et al., 2018). Due to the observed up-regulation of ILK kinase activity in post-anastatic cells, including the well-established connection between HIF-1α and EMT, it became a target of interest. Using

qPCR and western blotting techniques, it was determined that HIF-1α was highly up-regulated in post-anastatic cells, an intriguing result (Fig. 3.7 A-D).

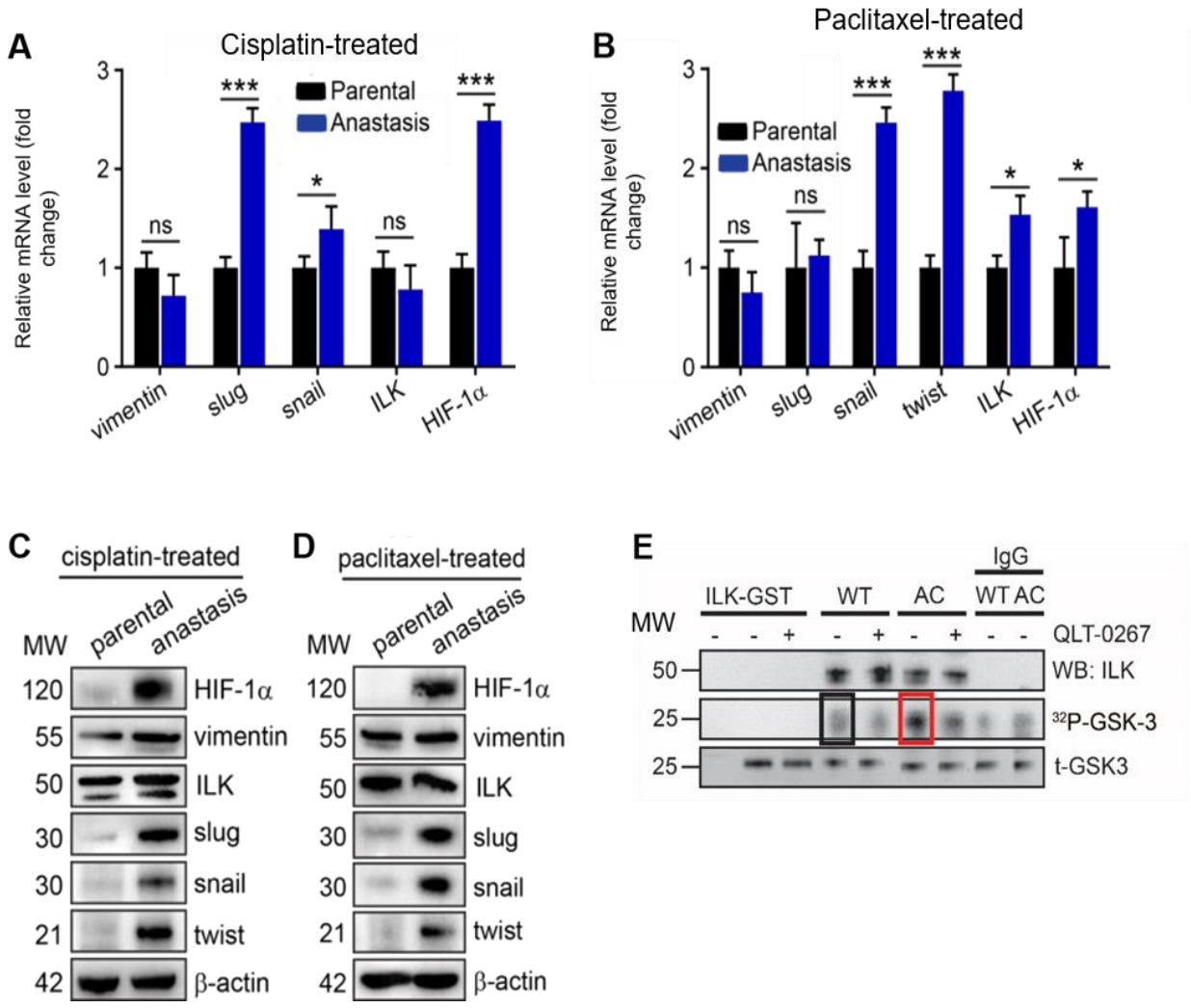

Fig. 3.7 Anastasis modulates signaling pathways involving EMT and hypoxic stress responses. (A-B) RT-qPCR analysis of EMT and hypoxic stress markers in SUM159PT-Cas3 cells, GAPDH served as an internal control. Data shows the mean ± s.e.m. of technical replicates (n=3-4/group) and are representative of three separate experiments *p≤0.05, ***p≤0.001. (A) Post-cisplatin induced anastasis. (B) Post-paclitaxel induced anastasis. (C-D) Western blot analysis of EMT and hypoxic stress markers in SUM159PT-Cas3 cells, β-actin served as a loading control. Results are representative of three separate experiments. (C) Post-cisplatin induced anastasis. (D) Post-paclitaxel induced anastasis. (E) Co-immunoprecipitation assessing ILK kinase activity in normal (WT) and cisplatin-treated post-anastatic (AC) SUM159PT cells. 3-hour exposure at -80°C.

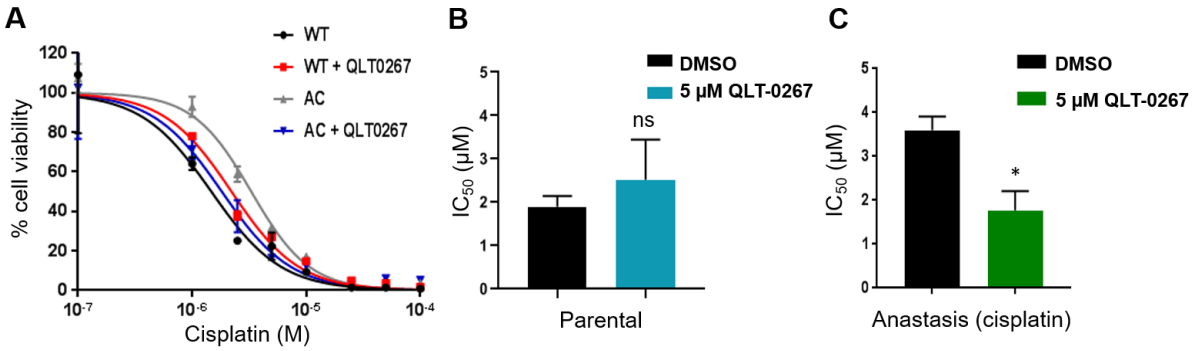

Figure 3.8 ILK inhibitor QLT-0267 results in the re-sensitization of post-anastatic cells to cisplatin. (A) Cell viability assay of parental and the anastasis line upon single and double treatment with a range of cisplatin (1 µM – 500 µM) and 5 µM QLT-0267. DMSO was used as a control. (B) IC_{50} (µM) of parental SUM159PT cells exposed to cisplatin alone or in combination with QLT-0267. Data shows the mean ± s.e.m. of technical replicates (n=4) and are representative of three separate experiments. ns= not significant. (C) IC_{50} (µM) of post-anastatic SUM159PT/AC cells exposed to cisplatin alone or in combination with QLT-0267. Data shows the mean ± s.e.m. of technical replicates (n=4) and are representative of three separate experiments *$p \leq 0.05$.

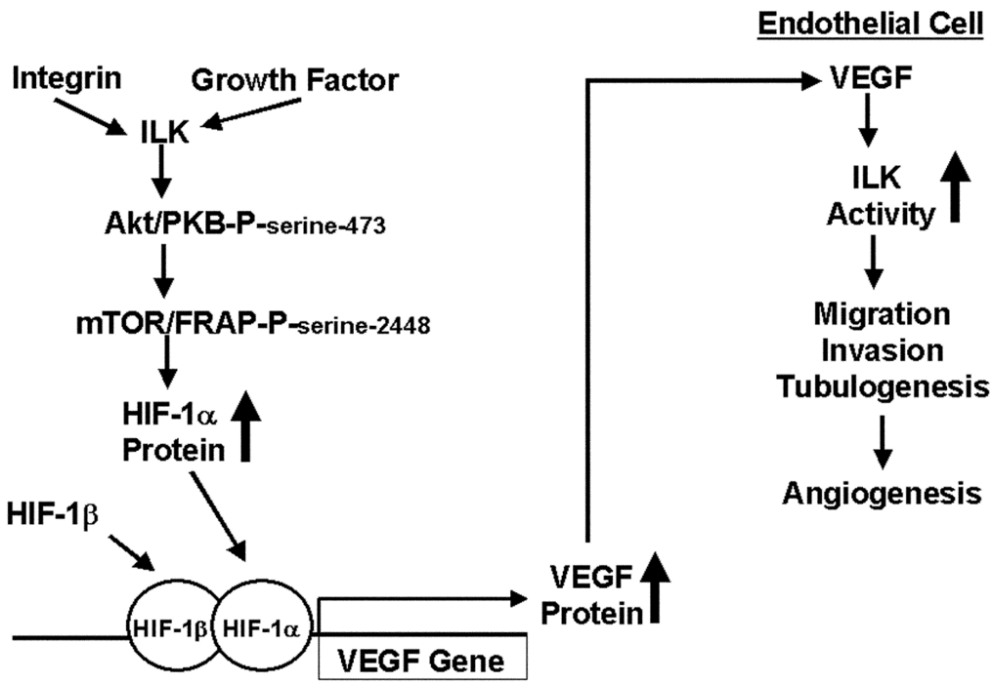

Figure 3.9 ILK regulates HIF-1α dependent up-regulation in normoxia through the PI3K/mTOR pathway. Schematic depicts the way in which ILK can lead to the up-regulation of HIF-1α under normoxic conditions, leading to a downstream up-regulation of proteins involved migration, invasion, and angiogenesis. Figure adapted from "Regulation of tumor angiogenesis by integrin-linked kinase (ILK)" (Tan et al., 2004).

3.2.2 Anastasis contributes to breast tumor invasion and metastasis *in vitro* and *in vivo*

As mentioned previously, EMT has been studied extensively where metastasis is involved, though it is not absolutely required for migration to occur. In light of the significant increase in associated EMT markers in post-anastatic cells, I wanted to investigate the possibility that cells having undergone anastasis were more invasive and metastatic. SUM159PT-Cas3 cells were cultured in an image-lock plate, where wounds were made and recorded using Incucyte ZOOM© and imaged at 2 h intervals over a period of 24 h. It was observed that post-anastatic cells were

more migratory than the parental cell line, with cisplatin-induced post-anastatic SUM159PT (AC) cells showing a 23% increase in the migration rate and paclitaxel-induced post-anastatic SUM159PT (AP) cells displaying a 34% increase (Fig. 3.10 A, B). Due to the increase in ILK kinase activity, as well as its known implications in the down-stream up-regulation of snail and slug, I wanted to investigate if an ILK inhibitor (QLT-0267) would have a significant effect on the rate of migration in the post-anastatic cell lines. It was observed that when treated with QLT-0267, the SUM159PT/AC cell line's migration decreased by 23%, while migration of the SUM159PT/AP cells decreased by 42%, completely abolishing the enhanced migratory propensity the cells originally possessed (Fig. 3.10. C-E). Due to the increase in migration, I wanted to determine if these cells also possessed an increased predisposition for invasion. Cells were incubated in serum-free media before being aliquoted into invasion chambers, which were then placed into a 24-well plate that contained media supplemented with EGF, acting as a chemical attractant, in order to promote cell invasion through the matrigel matrix. After incubating for approximately 18 h, they were fixed and stained with DAPI and imaged on a colibri microscope. The total number of cells per chamber having invaded through could be counted and analyzed. Similar to the migration data, post-anastatic cells were more invasive than their parental counterpart (Fig. 3.10 F).

To determine whether the increased invasive and migratory propensity *in vitro* was associated with a similar result *in vivo*, SUM159PT and SUM159PT/AC cells were orthotopically injected into the mammary fat-pad of female NSG mice. While both the parental and post-anastatic cells demonstrated similar growth rates and similar decline in weight, the post-anastatic cells not only showed an increased number of lymph-node metastases, but also produced large, secondary

tumors having invaded through the intraperitoneal muscle wall adjacent to the primary tumor; while, the parental cells produced no observable secondary tumors (Fig. 3.11 A-H). These results strengthen the observations that post-anastatic cells are significantly more metastatic and invasive both *in vitro* and *in vivo*.

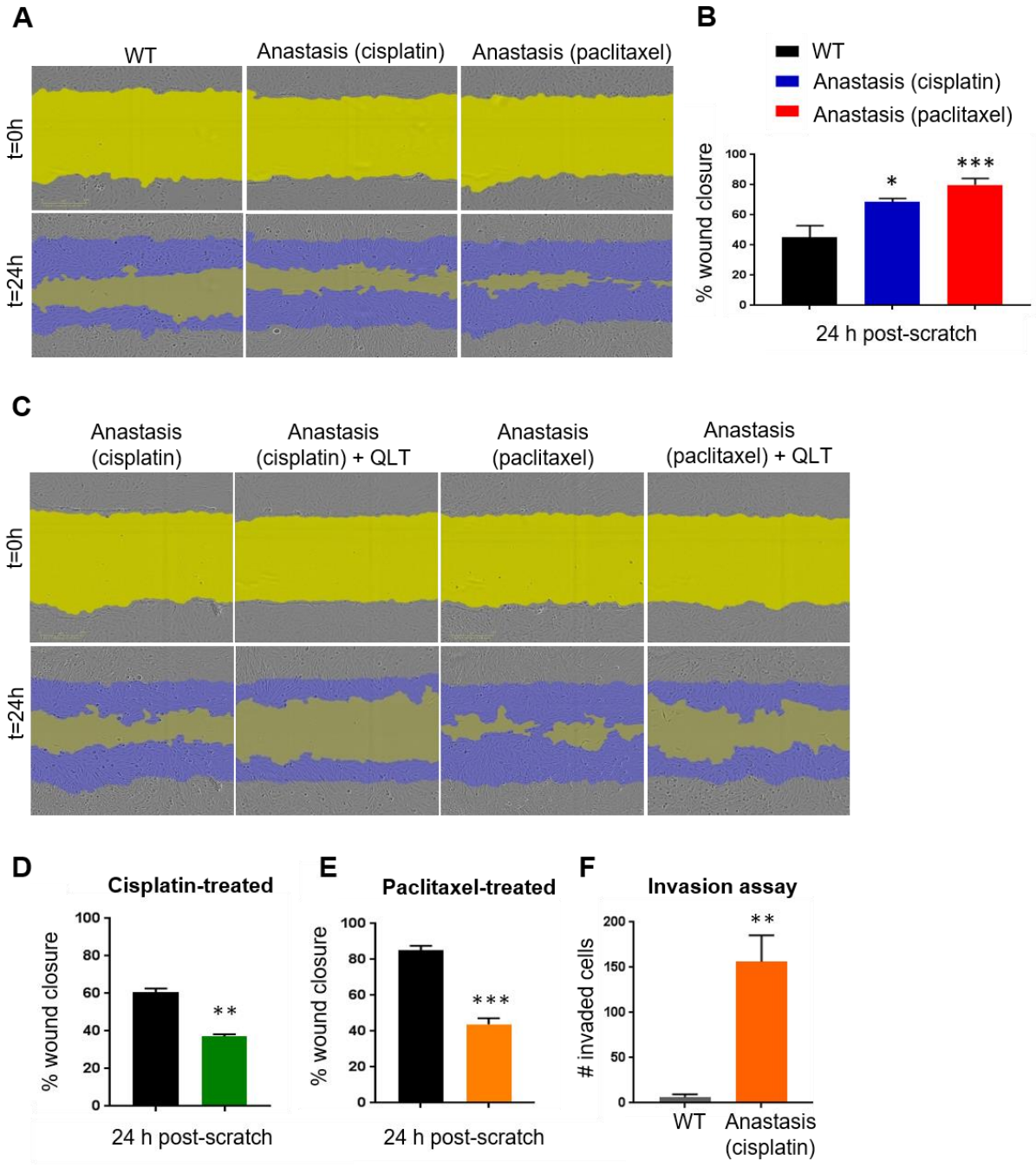

Fig. 3.10 Anastasis enhances migration and invasion of breast cancer cells *in vitro* through the regulation of ILK. (A) Images of a wound-induced cell migration by the parental and post-anastatic SUM159PT-Cas3 cells under normal conditions. Scale bar, 300 µm. The purple mask demarks the wound boundary at t=0 h, and the yellow mask as the wound area prior to cell migration. (B) Quantification of cell migration in A. Data shows the mean ± s.e.m. of technical replicates (n=6/group). *p≤0.05, ***p≤0.001. (C) Images of a wound-induced cell migration by the post-anastatic SUM159PT-Cas3 cells treated with 5 µM QLT-0267. Scale bar, 300 µm.

Wound-boundaries and cell-free area as previously described in A. (D-E) Quantification of cell migration in C. Data shows the mean ± s.e.m. of technical replicates (n=6/group). **p≤0.01, ***p≤0.001. (F) Quantification of boyden-chamber induced cell invasion of parental and post-anastatic SUM159PT-Cas3. Data shows the mean ± s.e.m. of technical replicates (n=6/group). **p≤0.01.

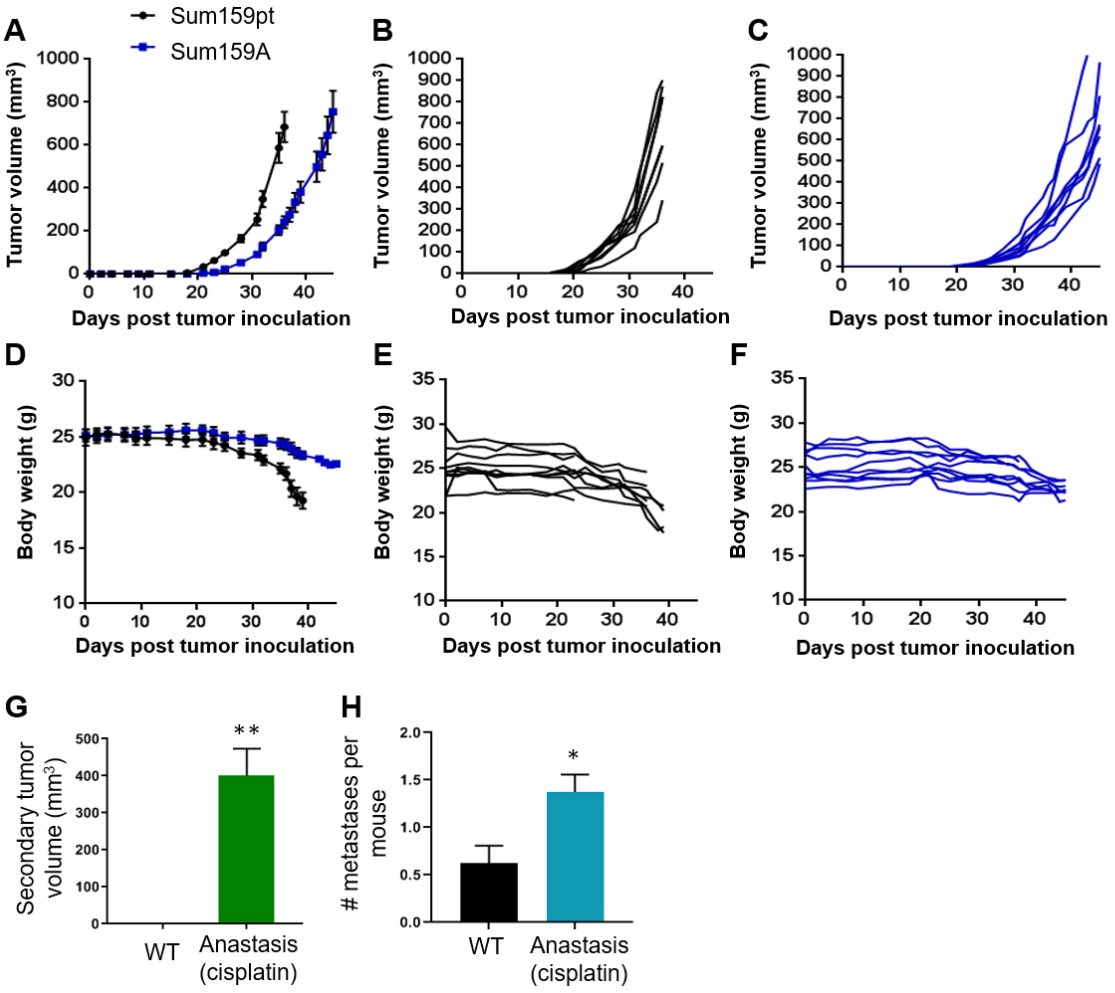

Fig. 3.11 *In vivo* growth kinetics of parental and post-anastatic SUM159PT cells injected into NSG mice show an increased invasive and metastatic phenotype. (A-C) Growth of tumors (mm^3) in mice over time (A) Mean ±sem of tumor volume (mm^3) in SUM159PT and SUM159PT/AC injected mice *(n=8/group).* (B) Tumor volume (mm^3) of individually SUM159PT injected mice *(n=8).* (C) Tumor volume (mm^3) of individually SUM159PT/AC injected mice *(n=8).* (D-E) Change in body weight (g) in mice over time. (D) Mean ±sem of body weight (g) in SUM159PT and SUM159PT/AC injected mice *(n=8/group).* (E) Body weight (g) of individually SUM159PT injected mice *(n=8).* (F) Body weight (g) of individually SUM159PT/AC injected mice *(n=8).* (G) Analysis of spontaneous secondary tumors having invaded through the intraperitoneal wall by SUM159PT cells following the growth of orthotopic breast tumors in NSG mice. Data shows the mean ±sem *n=8*/group. **p≤0.01. Statistical

analysis was performed using Welch's unpaired, two-tailed t-test. (H) Analysis of spontaneous lymph-node metastases by SUM159PT cells following the growth of orthotopic breast tumors in NSG mice. Data shows the mean ±sem *n=8*/group. **p≤0.01. Statistical analysis was performed using Welch's unpaired, two-tailed t-test.

3.2.3 Increased metabolic response under stress

Metastatic and invasive cancers associated with chemoresistance tend to have higher energy demands than those that do not, resulting in cachexia, or tissue wasting (Havas, K. M. et al., 2017). When it was determined that cells having undergone anastasis were more resistant and metastatic, I sought to determine if anastasis promotes an imbalance in energy consumption. In order to address this, I performed a Seahorse glycolysis stress test (Fig. 3.12 A). This experiment determined that post-anastatic cells possess not only increased glycolytic capacity, but also increased glycolytic reserve, and increased extracellular acidification under stress (Fig. 3.12 B & C). Moreover, there was an overall increase in the oxygen consumption rate in SUM159PT/AP, however, mitochondrial respiration would be a better indicator of this (Fig. 3.12 D). Additionally, post-anastatic cells, once again, are sensitive to the dual cisplatin and QLT-0267 treatment compared to the parental line. This exposure resulted in a dramatic dampening of the heightened glycolytic response (Fig. 3.10 E – H).

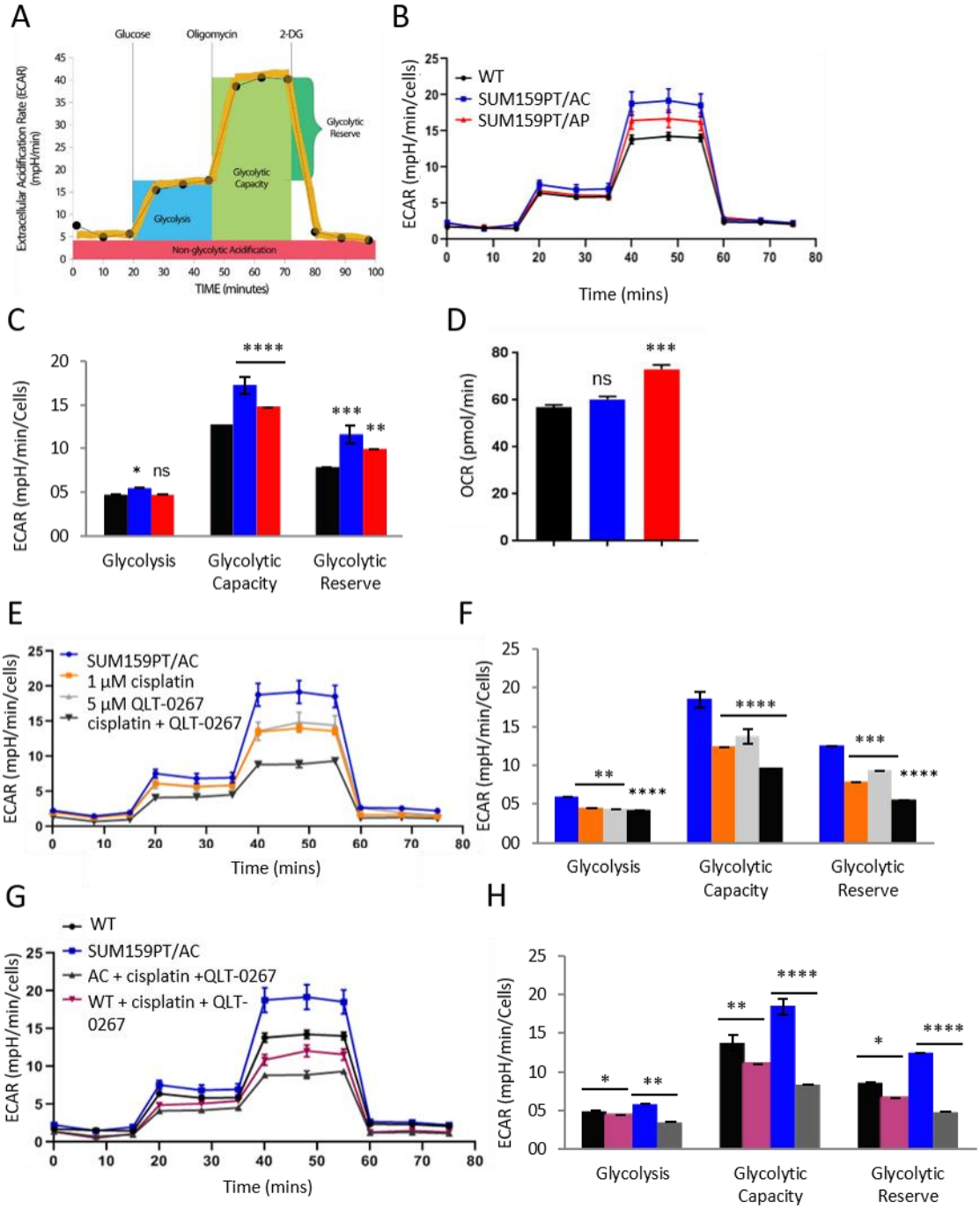

Fig. 3.12 Post-anastatic cells are more metabolically active in response to cellular stress. (A) Diagram depicting the glycolytic stress test profile, involving the treatment of glucose, oligomycin, and 2-DG at different timepoints in the experiment and how the various ECAR values are calculated. Figure is modified from "Agilent Seahorse XF Glycolysis Stress Test User Guide" (Agilent technologies, 2017). (B-H) Metabolic flux assay measuring the metabolic effects of cells under normal conditions and glycolytic stress. (B) Glycolytic stress test profile of SUM159PT, SUM159PT/AC, and SUM159PT/AP cell lines. (C) Analysis of results in (B),

including differences in glycolysis, glycolytic capacity and glycolytic reserve. *p≤0.05, **p≤0.01, ***p≤0.001, ****p≤0.0001. (D) Oxygen consumption rate of SUM159PT, SUM159PT/AC and SUM159PT/AP cell lines. ***p≤0.001. (E) Glycolytic stress test profile of SUM159PT/AC control and treated separately or combined dose of 1 µM cisplatin and 5 µM QLT-0267. (F) Analysis of results in (E), including differences in glycolysis, glycolytic capacity and glycolytic reserve. **p≤0.01, ***p≤0.001, ****p≤0.0001. (G) Glycolytic stress test profile of both SUM159PT and SUM159PT/AC control groups and groups treated with separate or combined dose of 1 µM cisplatin and 5 µM QLT-0267. (H) Analysis of results in (G) including, glycolysis, glycolytic capacity and glycolytic reserve. *p≤0.05, ***p≤0.001, ****p≤0.0001.

3.3 Potential mechanisms of anastasis

3.3.1 Decrease in caspase-3 activation

Executioner cas3 activation is essential throughout embryogenesis and many stages of human development. More specifically, the activation of cas3 plays multiple roles, including the progression of apoptosis by activating downstream effectors leading to the condensation of chromatin and DNA fragmentation. However, dysregulation of its activity can have harmful implications in the context of cancer. A decreased ability to cleave cas3 leads to a prevention in the procession of apoptosis and the assembly of the apoptosome, effectively preventing cell death. Due to the newly developed resistance in SUM159PT/AC post-anastatic cell line, I looked to examine whether these cell lines could evade cas3 activation when exposed to cisplatin and paclitaxel. In order to address this, I used western blotting analysis for total and cleaved levels of cas3. As expected, the post-anastatic cells had lower levels of activated cas3 (Fig. 3.13). In combination, the data shows that the post-anastatic cells are more resistant to the progression of end-stage apoptosis.

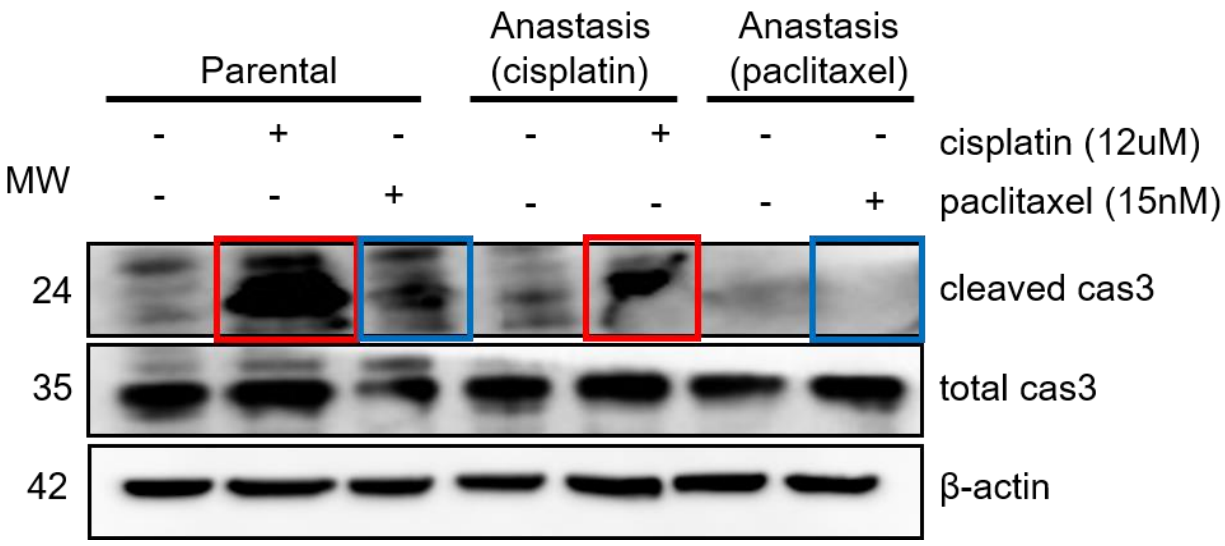

Fig. 3.13 Chemotherapy treatment results in decreased cas3 activation in post-anastatic cells. Western blot analysis of apoptotic markers in WT and post-anastatic SUM159PT cells. Cells were untreated or treated with 12 μM cisplatin or 15 nM paclitaxel. β-actin served as a loading control.

3.3.2 Alternatively-spliced caspase-3 isoform blocks apoptosis during early recovery

Due to the decrease in cas3 activation upon cytotoxic exposure, I sought to determine a mechanism through which this event was mediated. Previous studies have shown the existence of a caspase-3 isoform, caspase-3s. Caspase-3s (Cas3s) is a truncated form of the native pro-caspase-3 protein, where exon 6 is lost, resulting in the absence of the catalytic domain required for its cleavage and subsequent activation (Fig. 3.14) (Végran, F. et al., 2011). This prevents the initiation of cas3 activity and apoptosome assembly, thereby halting apoptosis. I sought to establish if cas3s was expressed in the post-anastatic cells. This was accomplished by using previously described cas3s primers for qPCR (Végran, F. et al., 2006). It was observed that cas3s

levels were 2 to 2.5-fold higher in both post-anastatic lines, strengthening the observation that post-anastatic cells may resist apoptotic initiation due to the increased presence of cas3s (Fig. 3.15 A).

The presence of cas3s lead me to examine if this isoform was involved during the recovery process of anastasis, when cells are recovering from end-stage apoptosis, or whether this was a long-term response. As a result, I performed a time-lapse recovery of cells undergoing anastasis in order to determine when the expression of cas3s occurs. This was accomplished by incubating parental SUM159PT-Cas3 cells in either paclitaxel or cisplatin for 18-24 h, thoroughly washing, and then allowing them to recover for a determined amount of time (0, 1, 2, 4, 6, and 8 h). Using RT-qPCR, I observed a time-dependent increase in the levels of cas3s, as well as a stable level of cas3 during recovery (Fig. 3.15 B-E). Additionally, using a pro-caspase-3 antibody, cas3s was detected through western blotting analysis in SUM159PT recovering after overnight cisplatin treatment (Fig. 3.15 F). This data points to a novel mechanism through which cells may be overcoming end-stage apoptosis and undergoing anastasis through the increase of cas3s.

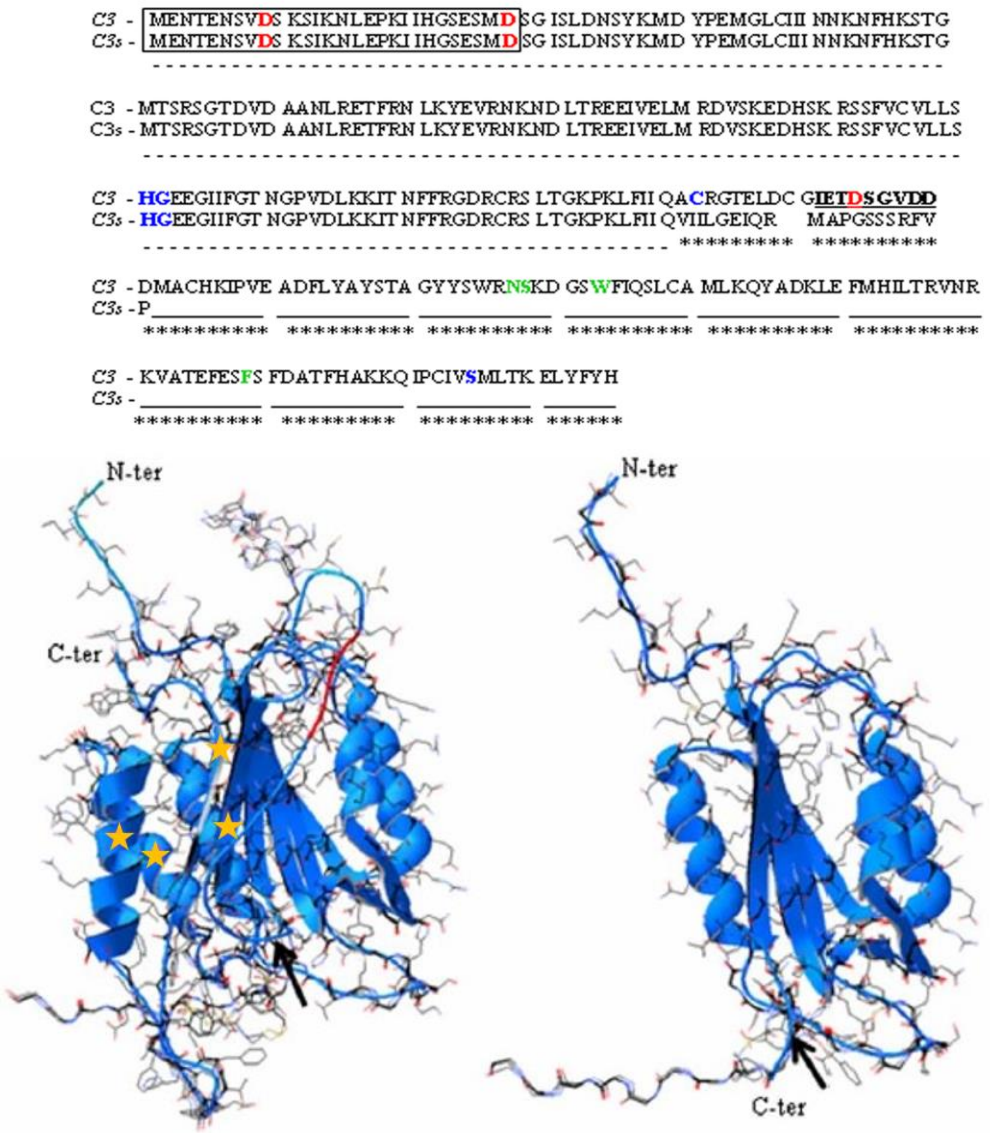

Fig. 3.14 The isoform cas3s is a truncated and catalytically inactive form of cas3. (A) Sequence alignment of cas3 (*top*) and cas3s (*bottom*) showing the missing sequence from exon 6. (B) Schematic depicting the structures of native cas3 (*left)* and cas3s isoform (*right*). Yellow stars on cas3 represents the two β-sheets and two α-helices missing from the isoform, which characterizes the catalytic domain, while the black arrow represents where the shared sequence ends. Figure is modified from "A Short Caspase-3 Isoform Inhibits Chemotherapy-Induced Apoptosis by Blocking Apoptosome Assembly" (Végran, F. et al., 2011).

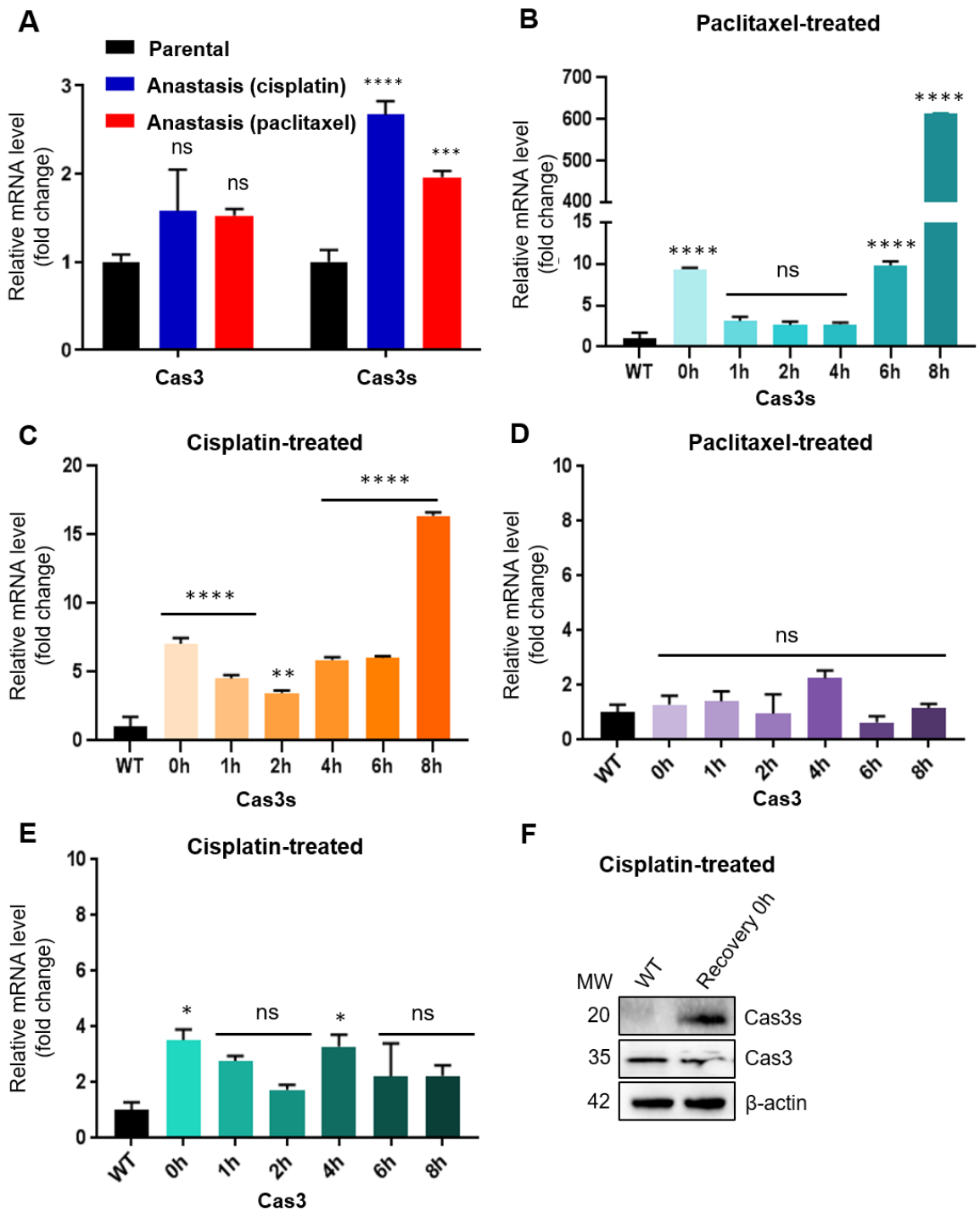

Fig. 3.15 A caspase-3 isoform blocks apoptosis in the early stages of anastasis after the removal of cytotoxic therapy. (A) RT-qPCR analysis of cas3 and cas3s in parental and post-anastatic (paclitaxel and cisplatin) SUM159PT-Cas3 cells. ***p≤0.001, ****p≤0.0001. Data shows the mean ±sem *n=4*/group. Two technical replicates were performed. **p≤0.01. (B) RT-qPCR analysis of cas3 after overnight treatment with 15 nM paclitaxel and the recovery in the

hours after the drug is removed. *p≤0.05, **p≤0.01, ****p≤0.0001. Data shows the mean ±sem *n=3*/group. Two technical replicates were conducted. **p≤0.01.(C) RT-qPCR analysis of cas3 after overnight treatment with 12 uM cisplatin and the recovery in the hours after the drug is removed. Data shows the mean ±sem *n=3*/group. Two technical replicates were conducted. **p≤0.01. (D) RT-qPCR analysis of cas3s after overnight treatment with 15 nM paclitaxel and the recovery in the hours after the drug is removed. Data shows the mean ±sem *n=3*/group. Two technical replicates were conducted. ****p≤0.0001. (E) RT-qPCR analysis of cas3s after overnight treatment with 12 μM cisplatin and the recovery in the hours after the drug is removed. Data shows the mean ±sem *n=3*/group. Two technical replicates were conducted. **p≤0.01, ****p≤0.0001. (F) Western blot analysis of Cas3 and Cas3s in SUM159PT WT and recovering cells at 0h timepoint after overnight treatment with 12 μM cisplatin.

Chapter 4: Conclusions and Future Directions

There are many proposed hypotheses for how chemoresistance arises in cancer cells, and it is well-known that metastasis and chemoresistance are highly coupled to one another. However, it is not well known how acquired chemoresistance relates to metastasis. The role of a newly discovered survival mechanism called “anastasis”, characterized by the reversal of end-stage apoptosis, is poorly understood, even more so pertaining to its role in potentiating survival in cancer cells after chemotherapy administration. Therefore, I sought to interrogate the role of anastasis during chemotherapy treatment of TNBC, and the mechanism by which this occurs.

In order to explore the effects of chemotherapy-induced anastasis, I needed to develop cancer cell models for identifying and tracking anastasis. I did so by using a Cas3 reporter that was transfected into the SUM159PT cell line. From this I could select for living cells, transiently treated with cisplatin or paclitaxel, with activated Cas3 using FACS. This allowed me to confidently assess that all cells that went on to survive and proliferate, had in fact undergone anastasis after end-stage apoptosis activation had occurred. I would like to mention that even though cells have the ability to undergo anastasis, that it is an incredibly rare event, with less than 1% of the population successfully surviving the activation of Cas3. Once recovered, post-anastatic cells possessed no obvious phenotypic differences from the parental line from which they were derived; once again highlighting the difficulty of recognizing post-anastatic cells.

4.1 Novel role of anastasis in TNBC

My initial focus was to determine whether chemotherapy-induced anastasis promotes resistance in TNBC. I was able to show that anastasis does in fact promote a significant increase in resistance to the original drug the cells were treated with. It was determined that the drug efflux pump MDR1 was not up-regulated in post-anastatic cells and therefore was not contributing to the acquired chemoresistance. However, in order to further strengthen these findings MRP3, another ATP-binding cassette efflux pump, should also be interrogated due to its relevance in breast cancer chemoresistance (Kool, M. et al., 1999; Scheffer, G. L. et al., 2002; Hinoshita, E. et al., 2000). Consequently, studies have demonstrated the connection between metastatic disease and acquired chemoresistance, therefore, I sought to determine if anastasis promotes migration and invasion (O'Reilly, E. A. et al., 2015; Fischer, K. R. et al., 2015). I established that post-anastatic cells are more migratory and invasive *in vitro* and more metastatic *in vivo*. Lastly, it is known that cancers that possess both metastatic and chemoresistant qualities tend to have higher energetic demands, therefore I wanted to assess any changes in metabolic activity in post-anastatic cells. My data shows that post-anastatic cells have a higher glycolytic capacity, glycolytic reserve, extracellular acidification rate, and increased oxygen consumption. This data is further supported by a recent study that produced cells having survived caspase-3 activation, without describing anastasis. They demonstrated that these cells possessed an up-regulated rate of lipid metabolism, in the form of β-oxidation, promoting tumor recurrence in breast cancer (Havas, K. M. et al., 2017). Therefore, interrogating the mitochondrial respiration of post-anastatic cells is a future experiment that will be conducted. To recapitulate, the phenotype that characterizes anastasis is supported by the established links between resistance, metastasis, and

metabolism, however, while this was very motivating, I sought to determine how anastasis resulted in this phenotype.

A previous study having performed a global screen of cells in the early recovery stages of anastasis have shown the presence of mRNA transcription factors such as snail, a prominent EMT marker, though its implications in anastasis are unclear (Sun, G. et al., 2017). This led us to explore the potential role of EMT and its involvement in newly acquired resistance. I discovered that a considerable number of EMT associated proteins, including snail, slug, and twist were up-regulated. The study also demonstrated an increase in the kinase activity of ILK in the SUM159PT/AC line and an increased presence of ILK mRNA in the SUM159PT/AP line. This was an interesting finding as a subpopulation of TNBC cells are already considered to possess a mesenchymal phenotype (Jeong, H et al, 2012) In addition, HIF-1α, a well-known twist interactor, was also found to be up-regulated both on the protein and mRNA level (Yang, M.-H. et al., 2008). This was surprising as it is typically only seen under hypoxic conditions where it can be stabilized. Previous studies have shown that under normoxic conditions, HIF-1α is involved in extra-cellular membrane (ECM) degradation and invasion in a variety of cancers. In addition, the role of HIF-1α in snail and twist activation is well known, especially concerning its role in metastasis (Yang, M.-H. et al., 2008). The mechanism through which HIF-1α promotes EMT, whether through hypoxia or overexpression, is by the direct binding of the twist promoter, that which up-regulates transcription and thus translation (Yang, M.-H. et al., 2008). Therefore, twist is an essential component to the induction of EMT through HIF-1α and may be why we see such a stark increase in mesenchymal markers in already highly mesenchymal cells (Yang, M.-H. et al., 2008). Additionally, there is increasing evidence supporting the up-regulation of HIF-

1α under normoxic conditions through the PI3K/mTOR pathway (Tan et al., 2004). Through this pathway, ILK mediates the expression of HIF-1α through the phosphorylation of Akt/PKB at the serine-473 position. This results in the downstream phosphorylation of serine-2448 on mTOR/FRAP resulting in the activation of mTOR/FRAP and subsequent up-regulation of HIF-1α translation. Additionally, there is enhanced expression of down-stream proteins involved in angiogenesis, metastasis, and invasion (Tan et al., 2004). A secondary study also depicted the relevance of the PI3K pathway in the expression of HIF-1α under normoxic conditions, through the activation of YB1, a DNA/RNA binding protein, responsible for binding HIF-1α mRNA directly in order to drive metastasis (Lefort et al., 2018). YB1 has been also been shown to bind the mRNA of slug and twist, resulting in the propagation of an EMT event in epithelial breast cells. Lastly, increased YB1 expression in tumors has been associated with poor patient survival, increased metastatic propensity, and chemotherapy resistance (Lefort et al., 2018). Considering the data that this research has produced and the importance of the PI3K pathway in normoxic HIF-1α regulation, future experiments will be concentrated on determining the potential involvement of PI3K in anastasis.

Due to the fact that ILK is a known up-stream regulator of snail and slug, I used a small molecule inhibitor, QLT-0267, in order to block its activity to determine its role in the post-anastatic phenotype. This led to the re-sensitization of SUM159PT/AC to cisplatin, without any notable effects on the parental cell line. These findings demonstrate that EMT may be a key regulator in the acquisition of chemoresistance driven by anastasis, moreover, this can be reversed once again through the pharmacological inhibition of ILK. It is worth noting that EMT is not always required for metastasis to occur, however it is highly correlated and appears to be

relevant in the context of anastasis. A similar effect was observed when post-anastatic cells were treated in combination with chemotherapy and QLT-0267. The enhanced metabolic phenotype was completely eliminated, all of which supports the idea that resistance and migration lead to an increase in the cellular energetic demand. However, more investigation is required in order to understand how resistance, metastasis, and metabolism are related in the context of anastasis.

As previously mentioned, anastasis is a rare cellular event and as a result is difficult to study. Due to the mechanism of action of cisplatin and paclitaxel, which require cells to actively divide, alongside the short incubation period that was required in order to collect the post-anastatic cells, it was expected that the yield of post-anastatic cells would be low (Horwitz, S. B., 1994; Siddik, Z. H., 2003). In addition to low cell yields, many were not able to survive active cas3, making this an increasingly difficult mechanism to study.

4.2 Novel mechanism driving anastasis

The data presented in my research describes, for the first time, a potential mechanism for how cells undergo anastasis, and how it plays an important role in mediating chemoresistance and metastasis. Previous studies led me to identify the presence of a cas3 isoform, cas3s, that was present in significantly higher levels in the post-anastatic cells long after recovery (Végran, F. et al., 2006). Cas3s is missing exon 6, which comprises the components of the catalytic domain found in native pro-cas3, and therefore it is unable to be cleaved by DEVDases. This results in an isoform that is inactive and cannot initiate apoptosome assembly. There are two proposed mechanisms by which this occurs, the first involves Cas3s binding to the activated procaspase-9/

apoptosome heterodimer resulting in the formation of a “short apoptosome” complex unable to cleave Cas3s (Végran, F. et al., 2011). The second proposed mechanism involves Cas3s binding Cas3, thereby preventing its binding to the apoptosome and subsequent cleavage.

In the hours after which anastasis is induced by the removal of the drug, the protein and mRNA cas3s levels rise rapidly, while cas3 levels remain relatively stable. This leads me to believe that cas3s functions in a dominate fashion over cas3 in order to prevent apoptosome assembly, allowing cells to survive. In fact, previous research has demonstrated the co-expression of cas3 and cas3s significantly decreased the ability for breast tumor cells to undergo apoptosis, further strengthening my findings (Végran, F. et al., 2006). These results were also corroborated by the decrease in cas3 cleavage when SUM159PT/AC and SUM159PT/AP cells were treated with cisplatin and paclitaxel, respectively. There is substantial evidence suggesting that deregulation of the spliceosome can result in the production of protein variants that promote tumorigenesis and the development of chemoresistance. Therefore, future experimentation should be focused on understanding how mRNA processing is shifting to produce cas3s and how we could potentially block its synthesis or target the mRNA product directly to prevent anastasis from occurring (Novoyatleva, T. et al., 2006).

In addition to this, future experimentation will include interrogating the cleavage of Cas3 more closely, specifically identifying the presence of the p10 fragment produced during cleavage. This will demonstrate any potential changes in Cas3 cleavage in post-anastatic cells. Lastly, Cas3s will be tagged in order to confirm the mechanism by which it prevents apoptosis and if this can be overcome by caspase-7 expression, an additional executioner caspase.

4.3 Relevance of anastasis in a clinical setting

The above data demonstrates a way in which cells can block apoptosis from occurring and acquiring resistance to the initial treatment. As a result, this may be an important indicator in the physiological response of a patient's tumor in a clinical setting. Treatment sessions are transient as to not harm the patient while still effectively targeting the tumor. Patients receive a certain number of treatments before going on what's known as a "drug holiday", where the patient ceases treatment for a period of time (Costa, A., 1993; Shenoy, R. S. et al., 1981; Kuczynski, E. A. et al., 2013). However, due to factors like chemotherapy dose, tumor size, and tumor blood supply, not all cells may be significantly impacted in a way required to induce committed cell execution. Moreover, when the treatment session is finished, the apoptotic stimulus is removed, giving cells the opportunity to overcome any current executioner caspase activity. Lastly, if a patient is considered "cancer free" due to undetectable cellular levels in the body, it is possible that dormant cells having undergone anastasis are waiting for more favorable cellular conditions to once again proliferate and decimate the body. All of these factors have the potential to result in the acquisition of resistance in already established tumors and in cases of relapse.

In the future, detecting anastasis in a clinical setting could be beneficial for determining personalized treatment plans for patients presenting with chemoresistant and metastatic disease. Patient biopsies could be used to detect the presence of anastasis by staining with a cas3s targeted antibody, if determined to be a suitable biomarker, or cleaved cas3, as well as using RNAseq in order to observe relevant shifts in RNA expression, such as EMT and hypoxia associated proteins slug, snail, twist, and HIF-1α.

4.4 Determining the role of the spliceosome in caspase-3s processing

The spliceosome is a large complex of ribonucleoproteins involved in the processing of pre-mRNA in the nucleus, through the excision of introns and the piecing together of exons, before its exportation to the cytoplasm for translation (Brinkman, B. M. N., 2004). Variants arise because exons can be joined in a variety of combinations to yield different downstream protein products. The mechanism through which this occurs is complex and involves the recognition of splices sites due to the binding of splicing factors and enhancers that flank the exon regions to be cut (Brinkman, B. M. N., 2004). Splicing plays an important role in explaining how complex mammalian organisms can produce so many gene products with so few genes (Brinkman, B. M. N., 2004). However, there is increasing evidence that variants are involved in the development and progression of cancer when dysregulated. This can result in the addition or removal of functional protein domains, altering its physiological function. Interestingly, in cases such as this, the variants can act to inhibit the function of the native protein product; for example, caspase-9 and Bcl-$_{xL}$ encode both pro and anti-apoptotic protein variants under diverse cellular conditions (Brinkman, B. M. N., 2004). This is one of the ways the cell can modulate protein activity, but if not tightly regulated, it can lead to the development and progression of cancer.

4.4.1 Targeting caspase-3s

Just like the above-mentioned variants, Cas3 has a pro-apoptotic and an anti-apoptotic variant and understanding the regulation between the production of one variant over another could give us insight into preventing its formation or targeting the mRNA products directly. In many

cancers, including breast, the increased presence of one isoform over the other is largely due to a mutation in RNA splicing factors. One of two scenarios arise as a result, either there is a global up-regulation of the gene in question, or the basal levels remain unchanged while the ratio for one isoform over another increases (Smith, M. A. et al., 2019).

Next steps for targeting Cas3s would first be to determine which RNA splicing factor, if any, is being affected, resulting in the truncation. Those associated with breast cancer are: SF3B1, SRSF2, U2AF1, U2AF2, SF1, SF3A1, and PRPF8, and could serve as targets for interrogation in future experimentation (Smith, M. A. et al., 2019). Additionally, there are RNA splicing inhibitors that can inhibit specific complexes of the spliceosome, including PlaB, CLK2, and EIF4A3 (Diouf, B. et al., 2018; Effenberger, K. A. et al., 2017; Carvalho, T. et al., 2017; Funnell, T. et al., 2017; Mazloomian, A. et al., 2019). There are limitations to this method, as alternative splicing plays an important role in producing many gene products in a healthy organism, and its hard to say what off-target effects could arise as a result of blocking the production of a variant in such a broad and general way. That being said, it is an excellent tool for studying the effects of the isoform *in vitro* as a proof of principle. In addition, because this isoform wreaks havoc by being non-functional, targeting the protein with an inhibitor is not a viable option. Therefore, it would be more meaningful to target the mRNA transcript with an oligonucleotide that could specifically bind the transcript, preventing translational machinery complex assembly, thus blocking the synthesis of the protein product (Kole, R. et al., 2012). This would be much more specific and prevent off-target effects of spliceosome targeted drugs.

The next steps for testing the importance of this variant during anastasis would be to target it, and then assess how the cells respond to subsequent chemotherapy treatment. *In vitro* this could be accomplished easily with an shRNA targeting the specific Cas3s sequence. In theory, diminishing the protective effects exerted by Cas3s would prevent anastasis from taking place. Additionally, Cas3s could be overexpressed in normal TNBC lines to show that this alone would cause a decrease in apoptotic activation without the original event of anastasis contributing, effectively linking the two events.

4.4.2 A biomarker of anastasis?

One of the difficulties of studying anastasis is the lack of a specific biomarker that identifies cells having undergone anastasis with certainty. For the purposes of *in vivo* research, biosensors are being developed that can permanently label cells having survived cas3 activation. However, in a clinical setting when studying tissues samples from patients, you cannot determine which cells have undergone anastasis, making it difficult to target patients for the treatment. Therefore, if cas3s is determined to be unique to post-anastatic cells, it could be used to as a biomarker in patients and targeted in order to optimize treatment strategies and effectiveness.

4.5 Characterizing the role of EMT and hypoxic stress markers in anastasis driven chemoresistance

It has been determined that EMT and hypoxic stress markers are playing some sort of functional role in maintaining resistance, migration, and invasion, that which can be reversed by ILK post-

anastasis. While this is an interesting observation, it tells us little about the interactions downstream from ILK, between the downstream EMT markers and HIF1-α, and how this is promoting the post-anastatic phenotype. Therefore, it is worth performing knock-outs of proteins such as ILK, slug, snail, twist, and HIF-1α in order to understand how other EMT associated protein signatures are affected, and how this in turn affects drug sensitivity, migration, and invasion. Additionally, demonstrating the effects of QLT-0267 and an ILK shRNA on downstream transcription factors snail and slug would strengthen EMTs involvement in anastasis. It would also be helpful to perform RNA-seq on cells having undergone anastasis to see what other interactors could be dysregulated that had not previously been considered in the context of anastasis long-term, as previous studies have only explored the early stages of recovery. This may expose key interactors with other pathways, such as PI3K, that had not been considered prior to the completion of this project.

4.6 Final thoughts

In conclusion, I have uncovered novel mechanisms for which anastasis-derived chemoresistance occurs. This data is the first to demonstrate that cells having undergone anastasis promote chemoresistance, migration, and invasion both *in vitro* and *in vivo*. Additionally, this project has provided new insight into a previously unknown mechanism through which anastasis recovery takes place and its role in the aftermath effects once recovery is complete. I have identified a target protein, ILK, that can reverse the effects of anastasis, a known regulator of EMT and the PI3K pathway, regarded as an important player in metastatic disease and resistance. Lastly, I have identified the presence of a cas3s splice variant that blocks apoptosome assembly and

apoptosis during the early stages of anastasis. The discovery of cas3s during anastasis not only serves as a potential mechanism, but also may serve as a potential biomarker for anastasis in the future. Further research in this field has the potential to bridge the gap between our understanding of the homeostasis between life and death as well as potentially improving the treatment and survival of patients with chemoresistant TNBC in the future.

References

Agilent Technologies (2017). *Agilent Seahorse XF Glycolysis Stress Test Kit*. Retrieved from https://www.agilent.com/cs/library/usermanuals/public/XF_Glycolysis_Stress_Test_Kit_User_Guide.pdf

Albini, A., & Sporn, M. B. (2007). The tumour microenvironment as a target for chemoprevention. Nat Rev Cancer, 7(2), 139–147. Retrieved from http://dx.doi.org/10.1038/nrc2067

Baer, H. J., Rich-Edwards, J. W., Colditz, G. A., Hunter, D. J., Willett, W. C., & Michels, K. B. (2006). Adult height, age at attained height, and incidence of breast cancer in premenopausal women. *International Journal of Cancer*, *119*(9), 2231–2235. https://doi.org/10.1002/ijc.22096

Bedi, A., Pasricha, P. J., Akhtar, A. J., Barber, J. P., Bedi, G. C., Giardiello, F. M., … Jj, R. J. (1995). *Inhibition of Apoptosis during Development of Colorectal Cancer1*. Retrieved from http://cancerres.aacrjournals.org/content/55/9/1811.full-text.pdf

Bosch, Ana, Pilar Eroles, Rosa Zaragoza,Juan R. Viña, and Ana Lluch. "Triple-negative Breast Cancer: Molecular Features, Pathogenesis, Treatment and Current Lines of Research." Cancer Treatment Reviews 36.3 (2010): 206-15.

"Breast Cancer Statistics - Canadian Cancer Society." www.cancer.ca. Web.

Brinkman, B. M. N. (2004). Splice variants as cancer biomarkers. *Clinical Biochemistry*, *37*(7), 584–594. https://doi.org/10.1016/J.CLINBIOCHEM.2004.05.015

Brown, N. S., & Bicknell, R. (2001). Hypoxia and oxidative stress in breast cancer Oxidative stress: its effects on the growth , metastatic potential and response to therapy of breast cancer.

Cahill, D. P., Lengauer, C., Yu, J., Riggins, G. J., Willson, J. K. V., Markowitz, S. D., … Vogelstein, B. (1998). Mutations of mitotic checkpoint genes in human cancers. *Nature*, *392*(6673), 300–303. https://doi.org/10.1038/32688

Carvalho, T., Martins, S., Rino, J., Marinho, S., & Carmo-Fonseca, M. (2017). Pharmacological inhibition of the spliceosome subunit SF3b triggers exon junction complex-independent nonsense-mediated decay. *Journal of Cell Science*, *130*(9), 1519–1531. https://doi.org/10.1242/jcs.202200

Chang, A. (2011). Lung Cancer Chemotherapy, chemoresistance and the changing treatment landscape for NSCLC. Lung Cancer, 71(1), 3–10.

Chen, W. Y., Rosner, B., Hankinson, S. E., Colditz, G. A., & Willett, W. C. (2011). Moderate Alcohol Consumption During Adult Life, Drinking Patterns, and Breast Cancer Risk. *JAMA*, *306*(17), 1884. https://doi.org/10.1001/jama.2011.1590

Cheng, G. Z., Chan, J., Wang, Q., Zhang, W., Sun, C. D., & Wang, L. (2007). Twist Transcriptionally Up-regulates AKT2 in Breast Cancer Cells Leading to Increased Migration , Invasion , and Resistance to Paclitaxel, (5), 1979–1987.

Cho, E., Chen, W. Y., Hunter, D. J., Stampfer, M. J., Colditz, G. A., Hankinson, S. E., & Willett, W. C. (2006). Red Meat Intake and Risk of Breast Cancer Among Premenopausal Women. *Archives of Internal Medicine*, *166*(20), 2253. https://doi.org/10.1001/archinte.166.20.2253

Colditz, G. A. (1998). Relationship Between Estrogen Levels, Use of Hormone Replacement Therapy, and Breast Cancer. *JNCI: Journal of the National Cancer Institute*, *90*(11), 814–823. https://doi.org/10.1093/jnci/90.11.814

Corden, B. J., Fine, R. L., Ozols, R. F., & Collins, J. M. (1985). Clinical pharmacology of high-dose cisplatin. *Cancer Chemotherapy and Pharmacology*, *14*(1), 38–41. https://doi.org/10.1007/BF00552723

Costa, A. (1993). Breast cancer chemoprevention. *European Journal of Cancer*, *29*(4), 589–592. https://doi.org/10.1016/S0959-8049(05)80158-3

Creighton, C. J., Chang, J. C., & Rosen, J. M. (2010). Epithelial-Mesenchymal Transition (EMT) in Tumor-Initiating Cells and Its Clinical Implications in Breast Cancer. https://doi.org/10.1007/s10911-010-9173-1

DeVita, V. T., & Chu, E. (2008). A History of Cancer Chemotherapy. Cancer Research, 68(21), 8643 LP-8653.

Diouf, B., Lin, W., Goktug, A., Grace, C. R. R., Waddell, M. B., Bao, J., … Jude, S. (2018). *Alteration of RNA splicing by small molecule inhibitors of the interaction between NHP2L1 and U4 HHS Public Access*. *23*(2), 164–173. https://doi.org/10.1177/2472555217735035

Dongre, A., & Weinberg, R. A. (2019). New insights into the mechanisms of epithelial–mesenchymal transition and implications for cancer. *Nature Reviews Molecular Cell Biology, 20*(2), 69–84. https://doi.org/10.1038/s41580-018-0080-4

Dunnwald, L. K., Rossing, M. A., & Li, C. I. (2007). Hormone receptor status, tumor characteristics, and prognosis: a prospective cohort of breast cancer patients. *Breast Cancer Research*, *9*(1), R6. https://doi.org/10.1186/bcr1639

Duque-Parra, J. E. (2005). Note on the Origin and History of the Term "Apoptosis". *The Anatomical Record.* https://doi.org/10.1002/ar.b.20047

Effenberger, K. A., Urabe, V. K., & Jurica, M. S. (2017). Modulating splicing with small molecular inhibitors of the spliceosome HHS Public Access. *Wiley Interdiscip Rev RNA*, *8*(2). https://doi.org/10.1002/wrna.1381

Ellis, N. A., & Norton, L. (2002). Outcome of Preventive Surgery and Screening for Breast and Ovarian Cancer in BRCA Mutation Carriers. *Article in Journal of Clinical Oncology*. https://doi.org/10.1200/JCO.20.5.1260

Ertürk, A., Wang, Y., and Sheng, M. (2014). Local pruning of dendrites and spines by caspase-3-dependent and proteasome-limited mechanisms. *J. Neurosci. 34,* 1672-1688.

Favaloro, B., Allocati, N., Graziano, V., Di Ilio, C., & De Laurenzi, V. (2012). Role of apoptosis in disease. *Aging*, *4*(5), 330–349. https://doi.org/10.18632/aging.100459

Fischer, K. R., Durrans, A., Lee, S., Sheng, J., Li, F., Wong, S. T. C., … Altorki, N. K. (2015). Epithelial-to-mesenchymal transition is not required for lung metastasis but contributes to chemoresistance. Nature, 527(7579), 472–476. https://doi.org/10.1038/nature15748

Fischer, Kari R. et al., "Epithelial-to-mesenchymal Transition Is Not Required for Lung Metastasis but Contributes to Chemoresistance." Nature 527.7579 (2015): 472-76.

Flanagan, L., Meyer, M., Fay, J., Curry, S., Bacon, O., Duessmann, H., … Prehn, J. H. M. (2016). Low levels of Caspase-3 predict favourable response to 5FU-based chemotherapy in advanced colorectal cancer: Caspase-3 inhibition as a therapeutic approach. *Cell Death & Disease*, *7*(2), e2087–e2087. https://doi.org/10.1038/cddis.2016.7

Fukumura, D., & Jain, R. K. (2007). Tumor microenvironment abnormalities: Causes, consequences, and strategies to normalize. *Journal of Cellular Biochemistry*, *101*(4), 937–949. https://doi.org/10.1002/jcb.21187

Funnell, T., Tasaki, S., Oloumi, A., Araki, S., Kong, E., Yap, D., … Aparicio, S. (2017). CLK-dependent exon recognition and conjoined gene formation revealed with a novel small molecule inhibitor. *Nature Communications*, *8*(1), 7. https://doi.org/10.1038/s41467-016-0008-7

Gyrd-Hansen, M., & Meier, P. (2010). IAPs: from caspase inhibitors to modulators of NF-κB, inflammation and cancer. *Nature Reviews Cancer*, *10*(8), 561–574. https://doi.org/10.1038/nrc2889

Havas, K. M., Sotillo, R., & Jechlinger, M. (2017). Metabolic shifts in residual breast cancer drive tumor recurrence The Journal of Clinical Investigation. *J Clin Invest*, *127*(6), 2091–2105. https://doi.org/10.1172/JCI89914

Helmbach, H., Kern, M. A., Rossmann, E., Renz, K., Kissel, C., Gschwendt, B., & Schadendorf, D. (2002). Drug Resistance Towards Etoposide and Cisplatin in Human Melanoma Cells is Associated with Drug-Dependent Apoptosis Deficiency. *Journal of Investigative Dermatology*, *118*(6), 923–932. https://doi.org/10.1046/J.1523-1747.2002.01786.X

Hinoshita, E., Uchiumi, T., Taguchi, K., Kinukawa, N., Tsuneyoshi, M., Maehara, Y., … Kuwano, M. (2000). Increased expression of an ATP-binding cassette superfamily transporter, multidrug resistance protein 2, in human colorectal carcinomas. *Clinical Cancer Research : An Official Journal of the American Association for Cancer Research*, *6*(6), 2401–2407. Retrieved from http://www.ncbi.nlm.nih.gov/pubmed/10873092

Holmes, M. D., Chen, W. Y., Feskanich, D., Kroenke, C. H., & Colditz, G. A. (2005). Physical Activity and Survival After Breast Cancer Diagnosis. *JAMA*, *293*(20), 2479. https://doi.org/10.1001/jama.293.20.2479

Hoon Jang, S., Guillaume Wientjes, M., Lu, D., & L-S Au, J. (2003). *Drug Delivery and Transport to Solid Tumors*. Retrieved from https://link.springer.com/content/pdf/10.1023%2FA%3A1025785505977.pdf

Horwitz, S. B. "Taxol (Paclitaxel): Mechanisms of Action." Annals of oncology : official journal of the European Society for Medical Oncology / ESMO, vol. 5 Suppl 6, 1994, pp. S3.

Hu, Q., Peng, J., Liu, W., He, X., Cui, L., Chen, X., … Wang, H. (2014). Elevated cleaved caspase-3 is associated with shortened overall survival in several cancer types. *International Journal of Clinical and Experimental Pathology*, *7*(8), 5057–5070. Retrieved from http://www.ncbi.nlm.nih.gov/pubmed/25197379

Hu, X., Stern, H. M., Ge, L., O'brien, C., Haydu, L., Honchell, C. D., … Cavet, G. (2009). Genetic Alterations and Oncogenic Pathways Associated with Breast Cancer Subtypes. *Mol Cancer Res*, *7*(4), 511–533. https://doi.org/10.1158/1541-7786.MCR-08-0107

Huang, H., Zhang, X.-F., Zhou, H.-J., Xue, Y.-H., Dong, Q.-Z., Ye, Q.-H., & Qin, L.-X. (2010). Expression and prognostic significance of osteopontin and caspase-3 in hepatocellular carcinoma patients after curative resection. *Cancer Science*, *101*(5), 1314–1319. https://doi.org/10.1111/j.1349-7006.2010.01524.x

Hypoxia/Normoxia. (2006). In Encyclopedic Reference of Genomics and Proteomics in Molecular Medicine (p. 853). Berlin, Heidelberg: Springer Berlin Heidelberg. https://doi.org/10.1007/3-540-29623-9_7440

Ilie, M., Hofman, V., Zangari, J., Chiche, J., Mouroux, J., Mazure, N. M., … Hofman, P. (2013). Response of {CAIX} and {CAXII} to in vitro re-oxygenation and clinical significance of the combined expression in {NSCLC} patients. Lung Cancer, 82(1), 16–25. https://doi.org/http://dx.doi.org/10.1016/j.lungcan.2013.07.005

Jeong, H., Ryu, Y., An, J., Lee, Y., & Kim, A. (2012). Epithelial-mesenchymal transition in breast cancer correlates with high histological grade and triple-negative phenotype. *Histopathology*, *60*(6B), E87–E95. https://doi.org/10.1111/j.1365-2559.2012.04195.x

Kalluri, R., & Weinberg, R. A. (2009). The basics of epithelial-mesenchymal transition. The Journal of Clinical Investigation, 119(6), 1420–1428. https://doi.org/10.1172/JCI39104

Kelly, W. K., Curley, T., Slovin, S., Heller, G., Mccaffrey, J., Bajorin, D., … Scher, H. (2001). Paclitaxel, Estramustine Phosphate, and Carboplatin Patients with Advanced Prostate Cancer. In *J Clin Oncol* (Vol. 19). Retrieved from http://citeseerx.ist.psu.edu/viewdoc/download?doi=10.1.1.977.4790&rep=rep1&type=pdf

Kenny, P. A., Lee, G. Y., & Bissell, M. J. (2007). Targeting the tumor microenvironment. *Frontiers in Bioscience : A Journal and Virtual Library*, *12*, 3468–3474. Retrieved from http://www.ncbi.nlm.nih.gov/pubmed/17485314

Kim, Yuri et al. "Hypoxic Tumor Microenvironment and Cancer Cell Differentiation." Current molecular medicine 9.4 (2009): 425–434. Print.

Kokkinos, M. I., Kang, M., & Newgreen, D. F. (2007). Vimentin and Epithelial-Mesenchymal Transition in Human Breast Cancer – Observations in vitro and in vivo, 191–203. https://doi.org/10.1159/000101320

Kole, R., Krainer, A. R., & Altman, S. (2012). RNA therapeutics: beyond RNA interference and antisense oligonucleotides. *Nature Reviews Drug Discovery*, *11*. https://doi.org/10.1038/nrd3625

Kool, M., van der Linden, M., de Haas, M., Scheffer, G. L., de Vree, J. M., Smith, A. J., … Borst, P. (1999). MRP3, an organic anion transporter able to transport anti-cancer drugs. *Proceedings of the National Academy of Sciences of the United States of America*, *96*(12), 6914–6919. https://doi.org/10.1073/pnas.96.12.6914

Kuczynski, E. A., Sargent, D. J., Grothey, A., & Kerbel, R. S. (2013). Drug rechallenge and treatment beyond progression—implications for drug resistance. *Nature Reviews Clinical Oncology*, *10*(10), 571–587. https://doi.org/10.1038/nrclinonc.2013.158

Lam, H., Man, H., Hou, K., Hu, S., Shan, S., & Man, K. (2011). Cell survival , DNA damage, and oncogenic transformation after a transient and reversible apoptotic response. https://doi.org/10.1091/mbc.E11-11-0926

Larue, L., & Bellacosa, A. (2005). Epithelial–mesenchymal transition in development and cancer: role of phosphatidylinositol 3′ kinase/AKT pathways. *Oncogene*, *24*(50), 7443–7454. https://doi.org/10.1038/sj.onc.1209091

Lefort, S., El-Naggar, A., Tan, S., Colborne, S., Negri, G. L., Pellacani, D., … Eaves, C. J. (2018). A Critical Role of Yb-1 in the Genesis and Progression of Kras-Mutated Human Breast Cancer. *BioRxiv*, 372524. https://doi.org/10.1101/372524

Liu, K.-Q., Liu, Z.-P., Hao, J.-K., Chen, L., & Zhao, X.-M. (2012). Identifying dysregulated pathways in cancers from pathway interaction networks. *BMC Bioinformatics*, *13*(1), 126. https://doi.org/10.1186/1471-2105-13-126

Liu, T., Xu, F., Du, X., Lai, D., Liu, T., Zhao, Y., Liu, Z. (2010). Establishment and characterization of multi-drug resistant, prostate carcinoma-initiating stem-like cells from human prostate cancer cell lines 22RV1. *Molecular and Cellular Biochemistry, 340*(1), 265–273. https://doi.org/10.1007/s11010-010-0426-5

London, S. J., Connolly, J. L., Schnitt, S. J., & Colditz, G. A. (1992). A Prospective Study of Benign Breast Disease and the Risk of Breast Cancer. *JAMA: The Journal of the American Medical Association*, *267*(7), 941. https://doi.org/10.1001/jama.1992.03480070057030

Ma, S., Pradeep, S., Hu, W., Zhang, D., Coleman, R., & Sood, A. (2018). The role of tumor microenvironment in resistance to anti-angiogenic therapy. *F1000Research*, *7*, 326. https://doi.org/10.12688/f1000research.11771.1

Martin, T. A., Goyal, A., Chb, M. B., Watkins, G., & Jiang, W. G. (2005). Expression of the Transcription Factors Snail , Slug , and Twist and Their Clinical Significance in Human Breast Cancer, 12(6), 1–9. https://doi.org/10.1245/ASO.2005.04.010

Mazloomian, A., Araki, S., Ohori, M., El-Naggar, A. M., Yap, D., Bashashati, A., … Aparicio, S. (2019). Pharmacological systems analysis defines EIF4A3 functions in cell-cycle and RNA stress granule formation. *Communications Biology*, *2*(1), 165. https://doi.org/10.1038/s42003-019-0391-9

Mbeunkui, F., & Johann, D. J. (2009). Cancer and the tumor microenvironment: a review of an essential relationship. *Cancer Chemotherapy and Pharmacology*, *63*(4), 571–582. https://doi.org/10.1007/s00280-008-0881-9

Mehlen, P., & Puisieux, A. (2006). Metastasis: a question of life or death. Nat Rev Cancer, 6(6), 449–458. Retrieved from http://dx.doi.org/10.1038/nrc1886

Minet, E., Michel, G., Remacle, J., & Michiels, C. (2000). Role of HIF-1 as a transcription factor involved in embryonic development, cancer progression and apoptosis (review). *International Journal of Molecular Medicine*, *5*(3), 253–262. https://doi.org/10.3892/ijmm.5.3.253

Mirzoeva, S., Kim, N. D., Chiu, K., Franzen, C. A., Bergan, R. C., & Pelling, J. C. (2008). Inhibition of HIF-1 alpha and VEGF expression by the chemopreventive bioflavonoid apigenin is accompanied by Akt inhibition in human prostate carcinoma PC3-M cells. Molecular Carcinogenesis, 47(9), 686–700. https://doi.org/10.1002/mc.20421

Modok, S., Mellor, H. R., & Callaghan, R. (2006). Modulation of multidrug resistance efflux pump activity to overcome chemoresistance in cancer. *Current Opinion in Pharmacology*, *6*(4), 350–354. https://doi.org/10.1016/J.COPH.2006.01.009

Molecular Classification of Breast Carcinomas by Comparative Genomic Hybridization: a Specific Somatic Genetic Profile for BRCA1 Tumors 1. (2002). In *CANCER RESEARCH* (Vol. 62). Retrieved from http://cancerres.aacrjournals.org/content/62/23/7110.full-text.pdf

Muggerud, A. A., Hallett, M., Johnsen, H., Kleivi, K., Zhou, W., Tahmasebpoor, S., … Wärnberg, F. (2010). Molecular diversity in ductal carcinoma in situ (DCIS) and early invasive breast cancer. *Molecular Oncology*, *4*(4), 357–368. https://doi.org/10.1016/j.molonc.2010.06.007

Novoyatleva, T., Tang, Y., Rafalska, I., & Stamm, S. (2006). *Alternative Splicing and Disease, "Pre-mRNA Missplicing as a Cause of Human Disease"*., 27-46. https://doi.org/10.1007/978-3-540-34449-0_2

O'Reilly, Elma A. et al. "The Fate of Chemoresistance in Triple Negative Breast Cancer (TNBC)." BBA Clinical 3 (2015): 257–275. PMC.

Putcha, G. V., Harris, C. A., Moulder, K. L., Easton, R. M., Thompson, C. B., & Johnson, E. M. (2002). Intrinsic and extrinsic pathway signaling during neuronal apoptosis. *J Cell Biol*, *157*(3), 441–453. https://doi.org/10.1083/JCB.200110108

Robson, M., Gilewski, T., Haas, B., Levin, D., Borgen, P., Rajan, P., … Offit, K. (1998). BRCA-associated breast cancer in young women. *Journal of Clinical Oncology : Official Journal of the American Society of Clinical Oncology*, *16*(5), 1642–1649. https://doi.org/10.1200/JCO.1998.16.5.1642

Rocha, C. R. R., Silva, M. M., Quinet, A., Cabral-Neto, J. B., & Menck, C. F. M. (2018). DNA repair pathways and cisplatin resistance: an intimate relationship. *Clinics (Sao Paulo, Brazil)*, *73*(suppl 1), e478s. https://doi.org/10.6061/clinics/2018/e478s

Saal, L. H., Gruvberger-Saal, S. K., Persson, C., Lövgren, K., Jumppanen, M., Staaf, J., … Borg, Å. (2008). Recurrent gross mutations of the PTEN tumor suppressor gene in breast cancers with deficient DSB repair. *Nature Genetics*, *40*(1), 102–107. https://doi.org/10.1038/ng.2007.39

Saramäki, O. R., Savinainen, K. J., Nupponen, N. N., Bratt, O., & Visakorpi, T. (2001). Amplification of hypoxia-inducible factor 1α gene in prostate cancer. *Cancer Genetics and Cytogenetics* (Vol. 128). Retrieved Online.

Saramäki, O. R., Savinainen, K. J., Nupponen, N. N., Bratt, O., & Visakorpi, T. (2001). Amplification of hypoxia-inducible factor 1α gene in prostate cancer. Cancer Genetics and Cytogenetics (Vol. 128). Retrieved Online.

Scheffer, G. L., Kool, M., de Haas, M., de Vree, J. M. L., Pijnenborg, A. C. L. M., Bosman, D. K., … Scheper, R. J. (2002). Tissue Distribution and Induction of Human Multidrug Resistant Protein 3. *Laboratory Investigation*, *82*(2), 193–201. https://doi.org/10.1038/labinvest.3780411

Serrano, I., Mcdonald, P. C., Lock, F., Muller, W. J., & Dedhar, S. (2013). Inactivation of the Hippo tumour suppressor pathway by integrin-linked kinase. Nature Communications, 4, 1–12. https://doi.org/10.1038/ncomms3976

Serrano, I., P. C. Mcdonald, F. E. Lock, and S. Dedhar. "Role of the Integrin-linked Kinase (ILK)/Rictor Complex in TGFβ-1-induced Epithelial–mesenchymal Transition (EMT)." Oncogene 32.1 (2013): 50-60.

Shahzina Kanwal. Effect of O-GlcNAcylation on tamoxifen sensitivity in breast cancer derived MCF-7 cells. Agricultural sciences. Université René Descartes - Paris V, 2013. English.

Shenoy, R. S., Sadler, A. G., Goldberg, S. C., Hamer, R. M., & Ross, B. (1981). Effects of a six-week drug holiday on symptom status, relapse, and tardive dyskinesia in chronic schizophrenics. *Journal of Clinical Psychopharmacology*, *1*(3), 141–145. Retrieved from http://www.ncbi.nlm.nih.gov/pubmed/6117584

Siddik, Zahid H. "Cisplatin: Mode of Cytotoxic Action and Molecular Basis of Resistance." Oncogene, vol. 22, no. 47, 2003, pp. 7265-7279 doi:10.1038/sj.onc.1206933.

Singhai, Rajeev et al. "E-Cadherin as a Diagnostic Biomarker in Breast Cancer." North American Journal of Medical Sciences 3.5 (2011): 227–233. PMC. Web.

Smith, M. A., Choudhary, G. S., Pellagatti, A., Choi, K., Bolanos, L. C., Bhagat, T. D., … Starczynowski, D. T. (2019). U2AF1 mutations induce oncogenic IRAK4 isoforms and activate innate immune pathways in myeloid malignancies. *Nature Cell Biology*, *21*(5), 640–650. https://doi.org/10.1038/s41556-019-0314-5

Sun, G., & Montell, D. J. (2017). *Q&A: Cellular near death experiences-what is anastasis?* https://doi.org/10.1186/s12915-017-0441-z

Sun, G., Guzman, E., Balasanyan, V., Conner, C. M., Wong, K., Zhou, H. R., … Montell, D. J. (2017). A molecular signature for anastasis, recovery from the brink of apoptotic cell death. *J Cell Biol*, *216*(10), 3355–3368. https://doi.org/10.1083/JCB.201706134

Supuran, C. T. (2008). Carbonic anhydrases : novel therapeutic applications for inhibitors and activators, 7(february). https://doi.org/10.1038/nrd2467

Tam, P. P. L., & Behringer, R. R. (1997). Mouse gastrulation: the formation of a mammalian body plan, 68, 3–25.

Tan, C., Cruet-Hennequart, S., Troussard, A., Fazli, L., Costello, P., Sutton, K., … Dedhar, S. (2004). Regulation of tumor angiogenesis by integrin-linked kinase (ILK). *Cancer Cell*, *5*(1), 79–90. https://doi.org/10.1016/S1535-6108(03)00281-2

Tan, E. Y. et al., "The Key Hypoxia Regulated Gene CAIX Is Upregulated in Basal-like Breast Tumours and Is Associated with Resistance to Chemotherapy." British Journal of Cancer 100.2 (2009): 405-11.

Tang, DM & Gururajan, R & J Kidd, V. (1998). Phosphorylation of PITSLRE p110 Isoforms Accompanies Their Processing by Caspases during Fas-mediated Cell Death. The Journal of biological chemistry. 273. 16601-7. 10.1074/jbc.273.26.16601.

Tang, H. M., & Tang, H. L. (2018). Anastasis: recovery from the brink of cell death. *Royal Society Open Science*, *5*(9), 180442. https://doi.org/10.1098/rsos.180442

Timmerman, L. A., Raya, A., Bertra, E., Dı, J., Aranda, S., Palomo, S., … Izpisu, J. C. (2004). Notch promotes epithelial-mesenchymal transition during cardiac development and oncogenic transformation, 5, 99–115. https://doi.org/10.1101/gad.276304.trol

Tomei, L.D.; Cope, F.O. *Apoptosis: The Molecular Basis of Cell Death*; Books on Demand: Stoughton, WI, USA, 1991.

"Treatments for breast cancer - Canadian Cancer Society." www.cancer.ca. N.p., n.d. Web

Ullah, M. S., Davies, A. J., & Halestrap, A. P. (2006). The Plasma Membrane Lactate Transporter MCT4, but Not MCT1, Is Up-regulated by Hypoxia through a HIF-1α-dependent Mechanism. Journal of Biological Chemistry, 281(14), 9030–9037. https://doi.org/10.1074/jbc.M511397200

Vasir, Jaspreet K., Labhasetwar, V. (2005). Targeted Drug Delivery in Cancer Therapy. *SAGE Journals*, *4*(4), 363–374. Retrieved from www.tcrt.org

Végran, F., Boidot, R., Oudin, C., Riedinger, J.-M., Bonnetain, F., & Lizard-Nacol, S. (2006). *Overexpression of Caspase-3s Splice Variant in Locally Advanced Breast Carcinoma Is Associated with Poor Response to Neoadjuvant Chemotherapy*. https://doi.org/10.1158/1078-0432.CCR-06-0725

Végran, F., Boidot, R., Solary, E., & Lizard-Nacol, S. (2011). A Short Caspase-3 Isoform Inhibits Chemotherapy-Induced Apoptosis by Blocking Apoptosome Assembly. *PLoS ONE*, *6*(12), e29058. https://doi.org/10.1371/journal.pone.0029058

Wan, Z., H. Pan, S. Liu, J. Zhu, W. Qi, K. Fu, T. Zhao, and J. Liang. 2015. Downregulation of SNAIL sensitizes hepatocellular carcinoma cells to TRA IL-induced apoptosis by regulating the NF-κB pathway. Oncol. Rep. 33:1560–1566.

Weigelt, B., Horlings, H., Kreike, B., Hayes, M., Hauptmann, M., Wessels, L., … Peterse, J. (2008). Refinement of breast cancer classification by molecular characterization of histological special types. *The Journal of Pathology*, *216*(2), 141–150. https://doi.org/10.1002/path.2407

Weigelt, B., Peterse, J. L., & van't Veer, L. J. (2005). Breast cancer metastasis: markers and models. *Nature Reviews Cancer*, *5*(8), 591–602. https://doi.org/10.1038/nrc1670

WHO | Risk factors. (2017). *WHO*. Retrieved from. https://www.who.int/topics/risk_factors/en/

Yang, J., & Weinberg, R. A. (2008). Review Epithelial-Mesenchymal Transition: At the Crossroads of Development and Tumor Metastasis. https://doi.org/10.1016/j.devcel.2008.05.009

Yang, M.-H., Wu, M.-Z., Chiou, S.-H., Chen, P.-M., Chang, S.-Y., Liu, C.-J., … Wu, K.-J. (2008). Direct regulation of TWIST by HIF-1α promotes metastasis. *Otolaryngology, and 6 Genomic Research Center, Taipei Veterans General Hospital*, *112*(201). https://doi.org/10.1038/ncb1691

Yang, M.-H., Wu, M.-Z., Chiou, S.-H., Chen, P.-M., Chang, S.-Y., Liu, C.-J., … Wu, K.-J. (2008). Direct regulation of TWIST by HIF-1α promotes metastasis. Otolaryngology, and 6 Genomic Research Center, Taipei Veterans General Hospital, 112(201). https://doi.org/10.1038/ncb1691

Youlden, D. R., Cramb, S. M., Dunn, N. A. M., Muller, J. M., Pyke, C. M., & Baade, P. D. (2012). The descriptive epidemiology of female breast cancer: An international comparison of screening, incidence, survival and mortality. *Cancer Epidemiology*, *36*(3), 237–248. https://doi.org/10.1016/J.CANEP.2012.02.007

Zhang, J., Wang, X., Cui, W., Wang, W., Zhang, H., Liu, L., … Li, B. (2013). Visualization of caspase-3-like activity in cells using a genetically encoded fluorescent biosensor activated by protein cleavage. *Nature Communications*, *4*(1), 2157. https://doi.org/10.1038/ncomms3157